

Article

Not peer-reviewed version

First-Principles Performance Verification of Gas-Solar Thermal Projects for Enhanced Oil Recovery

[Osama A. Marzouk](#)*

Posted Date: 3 November 2025

doi: 10.20944/preprints202511.0045.v1

Keywords: oil recovery; industrial; sustainability; thermal systems



Preprints.org is a free multidisciplinary platform providing preprint service that is dedicated to making early versions of research outputs permanently available and citable. Preprints posted at Preprints.org appear in Web of Science, Crossref, Google Scholar, Scilit, Europe PMC.

Copyright: This open access article is published under a Creative Commons CC BY 4.0 license, which permit the free download, distribution, and reuse, provided that the author and preprint are cited in any reuse.

Disclaimer/Publisher's Note: The statements, opinions, and data contained in all publications are solely those of the individual author(s) and contributor(s) and not of MDPI and/or the editor(s). MDPI and/or the editor(s) disclaim responsibility for any injury to people or property resulting from any ideas, methods, instructions, or products referred to in the content.

Article

First-Principles Performance Verification of Gas-Solar Thermal Projects for Enhanced Oil Recovery

Osama A. Marzouk

College of Engineering, University of Buraimi, Al Buraimi, Postal Code 512, Sultanate of Oman;
osama.m@uob.edu.om

Abstract

Tertiary oil recovery (TOR) is also called enhanced oil recovery. It is an industrial process used to extract additional crude oil that is difficult to extract using normal lifting techniques. Our study focuses on the use of solar thermal systems in Oman for sustainable oil recovery in Oman. In the presented solar thermal steam generation systems, arrays of parabolic troughs that are protected within glass houses are used to produce process steam for thermal oil recovery. The covered solar thermal systems in enhanced oil recovery are (1) Amal I, (2) Amal II, and (3) Miraah. Amal is the name of the oil field, which, when pronounced in Arabic, gives the meaning "hope". Miraah is the name of the oil field, which, when pronounced in Arabic, gives the meaning "mirror". These solar thermal steam generation systems can generate more than 2000 tonnes of steam per day, leading to a large reduction in the consumption of natural gas for fossil-based steam generation. We apply first principles and verify the heat demands and the carbon dioxide avoidance.

Keywords: oil recovery; industrial; sustainability; thermal systems

1. Nomenclature

ΔT	temperature rise
ρ	density of crude oil
ρ_r	density (bulk) of crude oil reservoir
AHU	air handling unit
AL	artificial lift
AOR	assisted oil recovery
$^{\circ}\text{API}$	American Petroleum Institute gravity degree
Bcf	billion standard cubic feet of natural gas (approximately equivalent to 1,000,000 MMBtu lower heating value "LHV")
CaCO_3	calcium carbonate
CF	capacity factor
C_r	representative specific heat capacity of a crude oil reservoir
DNI	direct normal irradiance
EOR	enhanced oil recovery (same as tertiary oil recovery, TOR)
ESEOR	enclosed solar enhanced oil recovery
GCR	ground coverage ratio
GHG	greenhouse gas
GWh	gigawatt-hour (equivalent to 3.6 TJ or 3.6×10^6 MJ)
HAPP	hydraulically activated pipeline pigging
IEA	International Energy Agency
L	reference length of a reservoir zone to be heated
LFR	linear Fresnel reflectors
LHV	lower heating value

MJ	megajoule (10^6 J)
MMBtu	million British thermal unit (equivalent to 1,055.1 MJ or 10 therms) [1,2]
MNm ³	million normal cubic meters of natural gas (approximately 35,000 MMBtu or 36,930 GJ lower heating value "LHV") ³
MWth	megawatt of thermal power
n	number of moles
NG	natural gas
NL	normal liter
Nm ³	normal cubic meter of natural gas (approximately 35,000 Btu or 36,930 kJ lower heating value "LHV")
OIIP	oil-initially-in-place
OOIP	original oil-in-place
OTSG	once-through steam generator [4–6]
p	absolute pressure
PDC	parabolic dish collector
PDO	Petroleum Development Oman
PJ	petajoule (quadrillion joules, 10^{15} J or 1,000 TJ)
ppb	part per billion
ppm	part per million
PTC	parabolic trough collector
Q	heat needed to increase the temperature of a reservoir zone
\bar{R}	universal (molar) gas constant, 8.3145 J/mol.K [7]
SCC	stress corrosion cracking
SEOR	solar enhanced oil recovery
SG	specific gravity
SHIP	solar heat for industrial processes
SOR	steam-oil ratio
T	absolute temperature
TDS	total dissolved solids
TEOR	thermal enhanced oil recovery
TES	total energy supply
TFC	total final consumption of energy
therm	10^5 Btu (equivalent to 0.1 MMBtu) [8,9]
TJ	terajoule (10^{12} J)
V	volume

2. Introduction

2.1. Importance of Sustainability for Oman

Recent studies show that the Sultanate of Oman is witnessing a verified trend of climate change, expressed as a steady increase in temperature at a rate of approximately 0.03 °C/year [10–12]. Hotter air can carry more moisture content, in accordance with the thermodynamic Clausius-Clapeyron relationship when applied to two-phase systems [13–15]. Therefore, this thermal anomaly can lead to interruptions in the natural hydrological cycle, reflected in heavy rainfalls and more frequent floods in Oman [16–18]. An example of the precipitation anomaly can be the exceptional April 2024 rainstorm accompanied by hail showers, heavy precipitation, and flash flooding that occurred in Oman and its neighboring country United Arab Emirates (UAE) [19,20].

Limiting the climate anomalies stems from curbing greenhouse gas (GHG) emissions [21], particularly carbon dioxide (CO₂) [22–24] through shifting from traditional practices in engineering and businesses to sustainable ones. Examples of such sustainability shifts [25] include phasing out systems and processes that rely heavily on burning fossil fuels [26,27], using electric propulsion (e-mobility) [28] in transportation [29–31], deploying green buildings that consume a small amount of energy [32,33], investing in green (zero-emissions) hydrogen and its derivatives [34–36], investing in

blue (low-emissions) hydrogen and its derivatives [37–39], exploring new high-performance power generation technologies [40–42], and encouraging the adoption of carbon capture technologies [43,44].

According to the International Energy Agency (IEA), the domestic energy production in Oman in 2022 was distributed as 59.3% crude oil (2,230,003 TJ), 40.6% natural gas (1,525,393 TJ), and 0.1% wind and solar energy (3,863 TJ) [45–48]. The term “domestic energy production” or (DEP) refers to all energy production (such as extracted fossil fuels), which can be used as fuels or burned to generate electricity [49], as well as energy produced by local nuclear reactors (not applicable in Oman) and renewable energy sources such as wind [50] and solar photovoltaic systems [51]. In terms of the Omani total energy supply (TES) profile in 2022; natural gas contributed the dominant share of 88.1% (1,023,964 TJ), while crude oil contributed a small share of 11.5% (134,165 TJ), and wind/solar energy contributed a marginal share of only 0.3% (3,863 TJ). The term “total energy supply” or (TES) refers to the result of subtracting all the energy that is exported outside a country or stored without immediate usage in that country from all the energy produced in that country or imported to it. In other words, the total energy supply (TES) represents the sum of all forms of energy that are needed to supply end users in the country [52,53]. Some of the energy sources involved in computing TES are used directly, whereas most of them are transformed into fuels or electricity for final consumption [54]. For the same year of 2022, electricity production in Oman depended on natural gas with a percentage of 94.7% (40,508 GWh), on crude oil with a percentage of 2.8% (1,190 GWh), and on the wind and solar photovoltaic systems with a percentage of 2.5% (1,073 GWh). In terms of the total final energy consumption (TFC) in Oman for 2022, natural gas represented 56.6% (600,340 TJ), oil products represented 31.1% (330,230 TJ), and electricity represented 12.3% (130,243 TJ). These energy mix figures are summarized in Table 1. They show the heavy penetration of fossil fuels in the Omani economy despite the abundance of clean energy resources [55–57]. This is a practice that the country aims to bring to a halt by 2050 [58]. This progress in sustainability and energy transition in Oman is aligned with progress in other domains [59–61], such as education [62–64] and urbanization [65], according to the Oman Vision 2040 [66–68].

Table 1. Energy mix in Oman, 2022.

Energy sector	Category 1 (largest)	Category 2 (intermediate)	Category 3 (smallest)
DEP (total: 3,759,259 TJ)	crude oil 59.3% 2,230,003 TJ	natural gas 40.6% 1,525,393 TJ	wind and solar 0.1% 3,863 TJ
TES (total: 1,161,992 TJ)	natural gas 88.1% 1,023,964 TJ	crude oil 11.5% 134,165 TJ	wind and solar 0.3% 3,863 TJ
Electricity generation (total: 42,771 GWh or 153,975.6 TJ)	natural gas 94.7% 40,508 GWh (145,828.8 TJ)	crude oil 2.8% 1,190 GWh (4,284 TJ)	wind and solar 2.5% 1,073 GWh (3,862.8 TJ)
TFC (total: 1,060,813 TJ)	natural gas 56.6% 600,340 TJ	oil products 31.1% 330,230 TJ	electricity 12.3% 130,243 TJ

2.2. Enclosed Solar Enhanced Oil Recovery (ESEOR)

One of the practices that is in need of sustainable transitioning in Oman is thermal enhanced oil recovery (TEOR), which is based on using steam. It is of special importance in Oman and similar oil-producing countries. In the current study, we present a case study of sustainable transitioning of the EOR in an oil field in Oman called “Amal” or “Amal West” [69,70]. In the original EOR process, natural gas was burned as the single source of heat energy to boil liquid water and convert it into hot steam suitable for underground injection to heat the crude oil and its surrounding rock layers,

rendering this crude oil less viscous and thus possible to extract. The modified EOR process utilizes collected solar radiation for clean steam generation, while still using natural gas for night operation. The current study provides an informative description of this hybrid EOR process, which is established by the company GlassPoint (or GlassPoint Solar) [71,72] for the company Petroleum Development Oman (PDO), which owns and operates that oil field [73–75].

GlassPoint is a private start-up business that started in 2009. It was funded by venture capital. The company specializes in designing and manufacturing solar steam generation units. The company went bankrupt and was liquidated in May 2020 in light of a challenging business environment related to low and unpredictable prices of oil and gas. However, the company restarted in June 2022 with a contract to build a gigawatt-scale solar steam project in Saudi Arabia for green aluminum production, where the solar steam is to be used this time for refining bauxite ore into alumina rather than thermal enhanced oil recovery [76].

Thermal steam-injection enhanced oil recovery (TEOR) requires supplying a large amount of heat to generate the hot steam. For example, recent computer modeling considered injecting superheated steam at 800 °F (426.67 °C) into the reservoir of heavy crude oil [77]. That modeling work reported that heating the reservoir from 100 °F (37.78 °C) [78,79] to 823.5 °F (439.72 °C) results in a big drop in the heavy oil viscosity from 9.940 Pa.s to 2.697 Pa.s, which improves the fluidity of the oil. To help realize the huge heat consumed in, we consider as an example a cubic foundation zone with a side length (L) of 100 m, which is to be heated by a reasonable temperature rise (ΔT) of 250 °C [80]. If the reservoir bulk (apparent) density (ρ_r) [81] is taken as 2,400 kg/m³ [82], and its specific heat capacity (C_r) is taken as 800 J/kg.K [83], and the volume is estimated as the cube of a reference characteristic length (L); then the thermal energy (Q) needed to raise the temperature of this reservoir zone is

$$Q = \rho_r L^3 C_r \Delta T \quad (1)$$

The above equation gives 480×10^{12} J or 480 TJ. This is equivalent to 133.3 GWh, which is enormous. It is equivalent to the electricity consumed if a large load of 15.22 MW; roughly as if 6,000 big residential air conditioning units are working simultaneously [84–88]; is kept running continuously over one full year (365 days or 8,760 hours).

In the solar enhanced oil recovery (SEOR) technique for the three Omani projects, parabolic trough mirror concentrators are used to collect and focus the incoming solar radiation for industrial heating, rather than for electricity generation [89–91]. Liquid water is heated and partly boiled to produce a two-phase liquid-vapor mixture “wet steam” with a quality of 80% [92] (a mixture of 80% water vapor and 20% liquid droplets) [93,94], at an absolute pressure [95] of about 100 bar (1,450 psi or 10 MPa) [96,97] and a saturation temperature of about 310 °C (583.15 K) [98]. This solar-generated steam is used to operate SEOR. The thermodynamic properties of steam at 100 bar absolute pressure are shown in Table 2 [99–101].

Table 2. Saturation properties of steam at 100 bar.

Property	Values		
	Saturated Liquid	Saturated vapor	Wet steam, 80% quality
Pressure	100 bar	100 bar	100 bar
Temperature	311.06 °C	311.06 °C	311.06 °C
Density	688.7052 kg/m ³	55.4754 kg/m ³	67.9754 kg/m ³
Specific volume	0.001452 m ³ /kg	0.018026 m ³ /kg	0.0147112 m ³ /kg
Specific internal energy*	1393.04 kJ/kg	2544.4 kJ/kg	2314.128 kJ/kg
Specific enthalpy [102]*	1407.56 kJ/kg	2724.7 kJ/kg	2461.272 kJ/kg
Specific entropy*	3.3596 kJ/kg.K	5.6141 kJ/kg.K	5.1632 kJ/kg.K

* The datum (zero reference values) corresponds to liquid water state at the triple point of water, 611.3 Pa and 0.01 °C [103,104].

For the three Omani projects covered here, the solar troughs are rotatable with one degree of freedom (DOF) to track the solar radiation [105,106], and they are placed in a greenhouse-like structure for protection from environmental disturbances and aerodynamic wakes [107–109], as well as to ease automated daily cleaning. This design leads to an enclosed solar enhanced oil recovery (ESEOR).

In enhanced oil recovery (EOR), unexploited crude oil (petroleum) in underground wells is pumped up with the aid of special oil production methods to reduce the flowing resistance of this oil and improve its extraction from the underground formation [110]. These special production methods for enhanced oil recovery (EOR) include injecting hot steam into the reservoir [111–114], thereby lowering the viscosity of the heavy viscous oil [115] (thermal thinning process), thus improving its ability to flow through the reservoir, or injecting a compressible miscible gas (such as carbon dioxide, CO₂) [116] through an injection well [117], and this external gas dissolves in the underground oil, thereby reducing its viscosity (miscible displacement process) [118] and improving its mobility [119,120].

The oil recovery stage that precedes EOR is called (secondary recovery) [121,122], which is, in turn, preceded by the initial stage of production that is called (primary recovery) [123,124]. In the first stage of crude oil recovery (namely, the primary recovery stage), the crude oil is naturally extracted under the initially high well pressure. During the primary recovery stage, it is possible to utilize mechanical pumping (mechanical lift process) using beam pumps (pump jacks) [125] or electric submersible pumps (ESP) [126], or inject an immiscible gas into the production tubing (gas lift process) [127] to artificially increase the well pressure [128]. This technique and system to boost the well pressure (head) for oil production during the primary recovery stage, if necessary, is referred to as (artificial lift) [129,130] or (AL) [131,132]. In the second stage of oil recovery (namely, the secondary recovery stage, taking place after the primary recovery stage, when the well pressure declines despite the artificial lift), the well is either flooded with incompressible liquid water (waterflooding process), such as by pumping seawater or brackish water, or a gas is injected (gas injection process) [133] into the gas cap [134], which is the accumulated gaseous zone at the upper part of the reservoir [135]. Either of these processes has the primary goal of maintaining the reservoir pressure [136,137], such that the oil production level remains high enough to render it economical.

A newly introduced term (assisted oil recovery) or (AOR) [138] can be used to refer to a condition where artificial lift is used during the primary oil recovery.

The amount of oil that can be recovered during each of the three production stages depends on the properties of the crude oil itself. For heavy oils, EOR is responsible for a large portion of the oil that can be produced from an oil field, as high as 90% of the original oil-in-place (OOIP) or oil-initially-in-place (OIIP), while only about 5% can be produced in either the first stage or the second stage [139]. On the other hand, for light oils, about 25% of the produced oil can be accomplished during either the first or second stage, with the remaining 50% accomplished during the third stage, which is the EOR stage [140].

Heavy oils can be defined as those having an American Petroleum Institute gravity degree (°API) below 22.3° [141,142], which corresponds to a specific gravity (SG) above 0.92 or a density (ρ) above 920 kg/m³. Heavy crude oils not only have relatively high densities, but also have high sulfur contents (an undesirable property) and high viscosities, causing resistance to flow (another undesirable property). Light oils can be defined as those having an °API > 31.1° [143,144] (SG < 0.87 or ρ < 870 kg/m³), and they are commercially desirable, due to the low sulfur content (making them easier to refine) and the low viscosities (making them easy to extract from the underground well) [145,146].

The API gravity degree is related to the specific gravity (SG) and the density (ρ) by the following nonlinear relationship [147]:

$$\rho = \frac{141,500}{^{\circ}\text{API} + 131.5} = 1,000 \text{ SG} \quad (2)$$

Figure 1 illustrates graphically the relationship between either density (ρ) or the specific gravity (SG) and the American Petroleum Institute gravity degree ($^{\circ}\text{API}$) over a range of $^{\circ}\text{API}$ between 10 and 50. This is wide enough to cover a large number of possible crude oils [148,149]. A quadratic regression model is also shown in the figure, which approximates the exact expression in the above equation well.

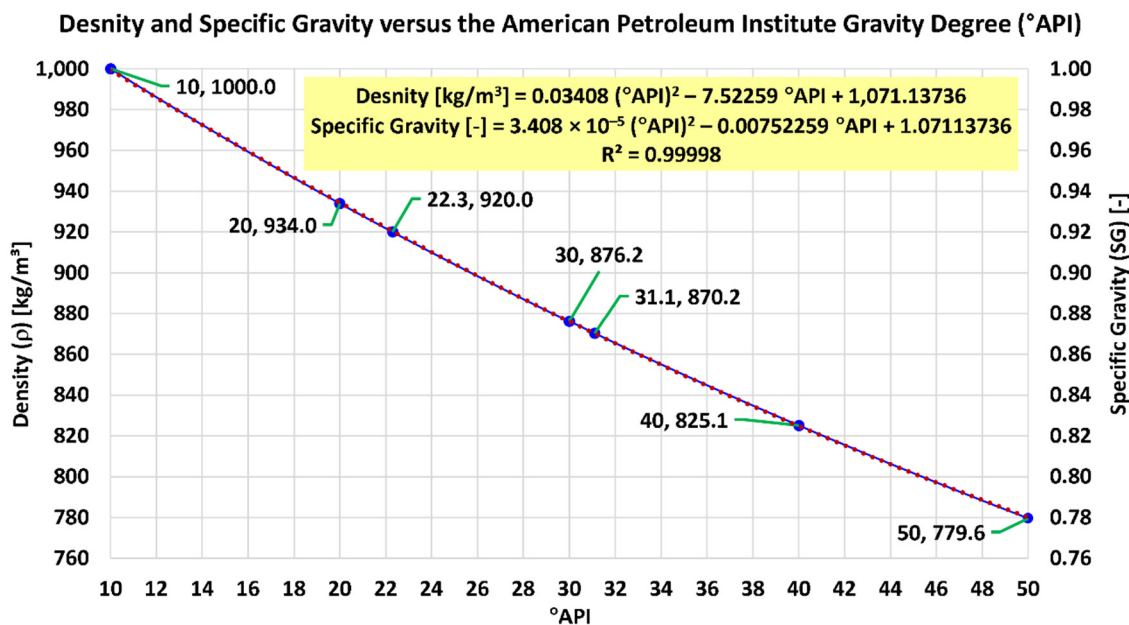


Figure 1. Relationship between the density or specific gravity and the American Petroleum Institute gravity degree.

The enclosed solar enhanced oil recovery (ESEOR) concept was implemented at either a pilot scale or a commercial scale for the first time in Oman at the Amal oil field. It is worth mentioning that a smaller test-scale or proof-of-concept (POC) unit was installed earlier in February 2011 in McKittrick, California, USA [150] (with a peak thermal capacity of 0.3 MWth or 300 kWth). Technically speaking, the McKittrick project of the GlassPoint company in California was the world's first enclosed solar enhanced oil recovery (ESEOR) project. However, the Miraah project in Oman is the world's first commercial-scale ESEOR project. Also, small scale, experimental scope, and limited monitoring records of the McKittrick project in California make it of secondary importance compared to the three subsequent ESEOR projects in Oman. Therefore, the current study can be of interest to readers and researchers working in the areas of enhanced oil recovery (EOR) and seeking information about this novel technology. The current study can attract the general interest of those working in solar thermal systems, solar heat for industrial processes (SHIP), and sustainability in the oil industry.

3. Research Methodology

3.1. Objectives and Contributions

The contributions of the current study to the literature of enhanced oil recovery, steam applications, solar heat for industrial processes (SHIP), and sustainable engineering practices include:

- Providing an example (a case study) of sustainable business operation in the oil industry. The current study is considered unique in terms of the provided independent technical and performance analysis of successful and flagship projects of enclosed solar enhanced oil recovery (ESEOR).
- Contrasting the three enclosed solar enhanced oil recovery (ESEOR) project designs in Oman, to derive best practices.

- Validating public data against first-principles models in a simple and reproducible way. Such validated data include avoided emissions of carbon dioxide (CO₂).
- Discussing general aspects and challenges of solar enhanced oil recovery (SEOR).

3.2. Approach and Data Sources

The research framework adopted in the current study is a case study analysis method, guided by qualitative and quantitative processing of secondary data. Supporting information was selected, cross-validated, organized, and presented such that it facilitates achieving the stated objectives of the current study.

Most of the data accessed about the three presented enclosed solar enhanced oil recovery (ESEOR) projects in Oman were made publicly available. The sources of these data can be categorized into three types as follows [151,152]:

- (1) The GlassPoint website.
- (2) Research publications by GlassPoint staff.
- (3) Personal communications with GlassPoint staff, through which further proprietary information was obtained.

4. Results and Discussions

The current section is dedicated to presenting our summary of the geometric and operational configurations for the three GlassPoint enclosed solar enhanced oil recovery (ESEOR) projects in Oman. All of them are geographically located in the same zone of the Amal oil field, which is an offshore petroleum reservoir in the southern part of Oman. These three projects are: Amal I (pilot scale), Amal II (pilot scale), and Miraah (commercial scale). The current section is divided into three subsections. In the first subsection, we provide a tabular comparison between the three ESEOR projects. In the second subsection, we provide graphical illustrations related to the ESEOR concept of GlassPoint. In the third subsection, we present photographs that help in depicting the real view of the three ESEOR projects in the field. In the fourth subsection, we discuss some aspects of operating the ESEOR projects. The attribution is properly made in the caption of each figure.

4.1. The Choice of Parabolic Trough Collectors

We start the results section by justifying the choice of parabolic trough collectors (PTC) as the solar heat collection design for all three GlassPoint enclosed solar enhanced oil recovery (ESEOR) projects in Oman. There are other options for solar heat collection, such as the linear Fresnel reflectors (LFR), the parabolic dish collector (PDC), and the solar tower. However, the parabolic trough collector (PTC) design has multiple attractive features, which are:

- Adequate temperature rise: Parabolic trough collectors can provide a broad range of high temperature rises (150–400 °C) [153–157], making them very suitable for solar steam generation.
- Maturity: Parabolic trough collectors are a very reliable technology that has been proven to be successful for many years, including large commercial-scale plants operating with stable conditions and low technological risks. A good example is the Mojave Solar project is a 250-megawatt solar electric generating facility (280 MW gross) in California, USA [158,159]. This commercial-scale PTC power plant has been operational for more than a decade (commissioned at the beginning of December 2014) [160].
- Modularity: Parabolic trough collectors are very scalable. They can be installed under a wide range of thermal capacities, ranging from a few kilowatts to hundreds of megawatts [161]. This makes them attractive for a diverse spectrum of industrial applications, including solar enhanced oil recovery.
- Simple construction: Parabolic trough collectors can be viewed as composed primarily of repetitive components (mirrors and receiver tube) and common materials (steel and glass) [162]. No large construction is needed (as in the case of the solar towers or the linear Fresnel reflectors).

Also, the one-dimensional solar tracking in the case of parabolic trough collectors [163] tends to be easier to maintain and install than the two-dimensional (two-angles) solar tracking in the case of parabolic dish collectors or the heliostats of a solar tower.

- Low cost: The structural simplicity and the maturity of parabolic trough collectors make them one of the lowest-cost solar options [164].
- Structural strength: The lack of high-rise structures and the layout in the form of parallel rows of reflective mirrors in parabolic trough collectors provides intrinsic structural strength [165–167] and suppresses airflow-induced vibrations [168,169].
- Effective land use: Compared to linear Fresnel reflectors (LFR) and solar towers, parabolic trough collectors (PTC) can permit better utilization of the available land area for the same power capacity.

It is useful to add here that in 2024, the largest investment for solar heat for industrial processes (SHIP) systems globally was for parabolic trough collectors (PTC), with a share of 66% in terms of the collector area or the equivalent thermal capacity [170].

Also, the superiority and dependability of the parabolic trough collectors (PTC) design is evidenced in selecting that design for building the world's largest solar steam generation project (1,500 MWth peak capacity and a solar field area of 6 km²) [171]. It is under construction in Saudi Arabia. The application sector is mining (aluminum production) [172,173] rather than the oil sector.

4.2. Contrasting the Three Enclosed Solar EOR Projects

In Table 3, we compare 15 characteristics for the three Omani ESEOR projects by GlassPoint Solar, and we also provide external references for additional information.

In addition, the receiver tube of the parabolic troughs is made of carbon steel, with all-welded construction and long-radius (less pressure loss) bends. It has an internal diameter of 48 mm and an external diameter of 60 mm. Also, solar steam is produced using a once-through steam generator (OTSG) system.

Computer ray trace modeling was used to inspect the optical behavior of the closely-packed parabolic trough collector mirrors in response to the changing sun position [174–176].

It can be noticed that the large scale Miraah project was built closer to the earlier Amal I project rather than the subsequent Amal II project (for example; by having gable roofs in both cases, adopting the same aperture size, and using unevacuated receiver tubes). The adopted flat roof glass in Amal I and Miraah is favored due to simplicity and lower cost compared to the curved glass roof in Amal II [177,178]. Similarly, the attempted evacuated tube (vacuum tube) design in Amal II is not repeated in the Miraah project (and was not implemented in Amal I). Such tube evacuation improves the performance through vacuum insulation that suppresses heat loss [179,180], but it implies a cost and installation penalty due to the incurred complexity.

Table 3. Comparison between the three GlassPoint enclosed solar enhanced oil recovery (ESEOR) projects in Oman.

Property	Amal I	Amal II	Miraah
1. Scale/purpose	Pilot	Pilot	Commercial
2. Thermal power capacity	8 MWth	8 MWth	330 MWth (initially planned as 1,021 MWth)
3. Annual heat energy output	12 GWh/year	12 GWh/year	445 GWh/year
4. Average daily steam output	50 tonnes	50 tonnes	2,000 tonnes

5. Solar field area	17,280 m ²	17,280 m ²	622,080 m ²
6. Total project area	46,200 m ²	46,200 m ²	781,200 m ²
7. Current status (as of mid-2025)	Dismantled	Dismantled	Operational (by PDO)
8. Construction starting year	2011	2018	2015
9. Steam production starting year	2012	2020	2017
10. Receiver tube evacuation	No	Yes	No
11. Number of trough rows and reflector mirrors	12 rows (3 mirrors per row)	16 rows (1 mirror per row)	3 modules (18 loops per module) (8 rows and 24 mirrors per loop) Thus, total: 432 rows (3 mirrors per row; thus, 1,296 mirrors)
12. Trough row size (length × aperture width)	60 m × 7.65 m	50 m × 7.32 m	60 m × 7.65 m
13. Shape of the greenhouse roof	gable	curve	gable
14. Annual natural gas savings	47,437 MMBtu/year (474,370 therms/year) (13.902 GWh/year) (0.05005 PJ/year) (0.047437 Bcf/year) (1.3553 MNm ³ /year)	47,437 MMBtu/year (474,370 therms/year) (13.902 GWh/year) (0.05005 PJ/year) (0.047437 Bcf/year) (1.3553 MNm ³ /year)	1,897,461 MMBtu/year (18,974,610 therms/year) (556.091 GWh/year) (2.00193 PJ/year) (1.897461 Bcf/year) (54.2132 MNm ³ /year)
15. Annual CO ₂ emissions avoided	2,514 tonnes/year	2,514 tonnes/year	100,565 tonnes/year
References	[181–183]	[184]	[185,186]

The above results of the reduced natural gas consumption are aligned with a reduction of about 25% of the original system. Thus, the capacity factor (CF), or the ratio of actual output heat compared to the theoretical output heat assuming continuous operation at the peak rated power [187,188], of the enclosed solar enhanced oil recovery (ESEOR) design is about 25%. This can be justified by the absence of solar radiation at night, and the weakened absorbed radiation outside the solar noon time, partly due to self-shading [189,190] and partly due to gradually weakened direct normal irradiance

(DNI) [191,192]. It is useful to add here that such a low capacity factor is usual for solar systems [193–195].

Summing the amount of annually avoided natural gas consumption gives the following figures in Table 4.

Table 4. Total avoided natural gas (NG) consumption if the three ESEOR projects are operated simultaneously.

Unit	Summed annual avoided NG (three projects together)
MMBtu/year	1,992,335
therms/year	19,923,350
GWh/year	569.993
PJ/year	2.05198
Bcf/year	1.992335
MNm ³ /year	56.9238

Similarly, the summed annual avoided carbon dioxide emissions from the three ESEOR projects are 105,593 tonnes/year.

4.3. Thermal and Emissions Validation Model

To validate the heat and CO₂ emissions values reported in the previous subsection (as reported by third-party sources), we provide here a simple thermal and emissions validation model [196] to verify these values in terms of their magnitude. We found that these values are acceptable as explained below.

The latent heat of vaporization or enthalpy of vaporization (the energy needed to convert 1 kg of saturated liquid water to saturated water vapor) at this pressure is 1,317.1 kJ/kg(water) or 0.36586 kWh/kg(water). Sensibly heating water from ambient temperatures to 310 °C requires an additional specific heat of about 1,425.4 kJ/kg(water) or 0.39594 kWh/kg(water). Summing both types of heats gives 2,742.5 kJ/kg, 0.76180 kWh/kg(water), or 2.5993 MMBtu/tonne(water).

Therefore, producing 1 tonne of steam daily during one year (365 days) requires a heat of about 948.7445 MMBtu or 1,000.98 GJ. Producing 50 tonnes of steam daily during one year (365 days) requires a heat of about 47,437 MMBtu or 50,049 GJ. This estimated quantity is identical to the GlassPoint-reported value of 47,437 MMBtu/year for either the Amal I pilot project or the Amal II pilot project, as shown in Table 3. Producing 2,000 tonnes of steam daily during one year (365 days) requires a heat of about 1,897,489 MMBtu or 2,001,960 GJ. This estimated quantity is very close to the GlassPoint-reported value of 1,897,461 MMBtu/year for the Miraah full-scale project, as shown in Table 3.

Because natural gas has a lower heating value (LHV) of approximately 0.035 MMBtu/Nm³ (0.03693 GJ/Nm³ or 10⁶ MMBtu/Bcf), producing 1 tonne of steam daily during one year (365 days) requires burning about 27,106 Nm³ (0.027106 MNm³ or 0.0009487445 Bcf) of natural gas. Producing 50 tonnes of steam daily during one year (365 days) requires a heat of about 1.3553 million Nm³ (1,355,300 Nm³ or 0.047437 Bcf) of natural gas. Producing 2,000 tonnes of steam daily during one year (365 days) requires a heat of about 54.212 million Nm³ (54,212,000 Nm³ or 1.897 Bcf) of natural gas.

The reasonable and equivalent carbon dioxide emission factors for natural gas [197] of 52.9996 kg(CO₂)/MMBtu, 185,253 kg(CO₂)/GWh, 185.253 kg(CO₂)/MWh, 0.185253 kg(CO₂)/kWh, 51.4591 kg(CO₂)/GJ, 0.0514591 kg(CO₂)/MJ, 52,999,621 kg(CO₂)/Bcf(NG), 1,854,989 kg(CO₂)/MNm³(NG), and 1.854989 kg(CO₂)/Nm³(NG); it can be computed that producing 1 tonne of steam daily during one year (365 days) by burning natural gas results in CO₂ emissions of 50,283.1 kg. Producing 50 tonnes

of steam daily during one year (365 days) by burning natural gas results in CO₂ emissions of 2,514,155 kg. This estimated quantity is identical (when the same number of significant digits is compared) to the GlassPoint-reported value of 2,514 tonnes(CO₂)/year for either the Amal I pilot project or the Amal II pilot project, as shown in Table 3. Producing 2,000 tonnes of steam daily during one year (365 days) by burning natural gas results in CO₂ emissions of 100,566,200 kg. This estimated quantity is close to the GlassPoint-reported value of 100,565 tonnes(CO₂)/year for the Miraah full-scale project, as shown in Table 3.

With regard to the above-quoted carbon intensity, the following theatrical justification can be made. Natural gas consists mainly of methane (CH₄) [198], with a molar fraction of around 95% [199]. The ideal stoichiometric reaction of methane [200] with oxygen is



Thus, in terms of moles, the perfect combustion of one mole of methane leads to the emission of one mole of carbon dioxide (CO₂). The molecular weight of methane is approximately 16 kg/kmol [201], and the molecular weight of carbon dioxide is approximately 44 kg/kmol [202]. Therefore, the perfect combustion of 1 kg of methane leads to the emission of 2.75 kg(CO₂), or 44/16 kg(CO₂). The volumetric lower heating value (LHV) of natural gas is approximately 35,000 Btu/Nm³ or 36,930 kJ/Nm³ [203]. Treated as an ideal gas [204], one mole (kmol) of methane or natural gas at 15 °C and 1 atm or 101,325 Pa [205] occupies about 23.645 normal liters (NL) and has a mass of approximately 16 g. This can be derived using the following ideal gas law:

$$V = n \bar{R} T/p \quad (4)$$

In the above equation, setting the number of moles (n) to 1, the universal (molar) gas constant (\bar{R}) to 8.3145 J/mol.K [206], the absolute temperature (288.15 K) that corresponds to 15 °C, and the absolute pressure (p) to 101,325 Pa, gives the standard volume of 0.023645 normal cubic meters (Nm³) or 23.645 normal liters (NL).

Therefore, one kilomole (kmol) of methane or natural gas occupies about 23.645 Nm³ and has a mass of approximately 16 kg at normal conditions. Thus, one normal cubic meter of methane (or natural gas) has an LHV energy content of 35,000 Btu/Nm³ (or 36,930 kJ/Nm³) × 23.645 Nm³/kmol, which results in 827,575 Btu/kmol(CH₄) or 873,209.85 kJ/kmol(CH₄). Given the 1:1 molar ratio between methane and carbon dioxide, these energy intensities can be converted into reciprocal carbon intensities as 0.827575 MMBtu/kmol(CO₂) or 0.87320985 GJ/kmol(CO₂). Converting these molar reciprocal carbon intensities into mass-based (gravimetric) reciprocal carbon intensities via dividing by the molecular weight of carbon dioxide (44 kg/kmol) gives 0.0188085 MMBtu/kg(CO₂) or 0.0198457 GJ/kg(CO₂). Taking the reciprocal of these values gives estimated ideal carbon intensities for natural gas combustion as 53.1674 kg(CO₂)/MMBtu or 50.3888 kg(CO₂)/GJ. Given that 1 MWh = 3.6 GJ = 3,600 kWh, our estimated carbon intensity is also equivalent to 181.400 kg(CO₂)/MWh and 0.181400 kg(CO₂)/kWh. These estimates are very close to the reported third-party value.

4.4. Illustrative Sketches

To explain the geographical location of the Amal field (and thus the three ESEOR projects covered here), Figure 2 has a useful map that demonstrates this [207]. The oil field is located in the southern part of Oman. The Amal oil field is in the north of the Dhofar governorate (the southern governorate of Oman), near its north border with the neighboring "Al Wusta" governorate (the central governorate of Oman). The field is located about 50 km north of the Arabian Sea coast.

The Amal oil field is located at the geographic coordinates of 18.3333989° North, 55.6684729° East [208].

The Miraah enclosed solar enhanced oil recovery (ESEOR) project is located at a latitude of 18.349281° North and a longitude of 55.684590° East [209,210].

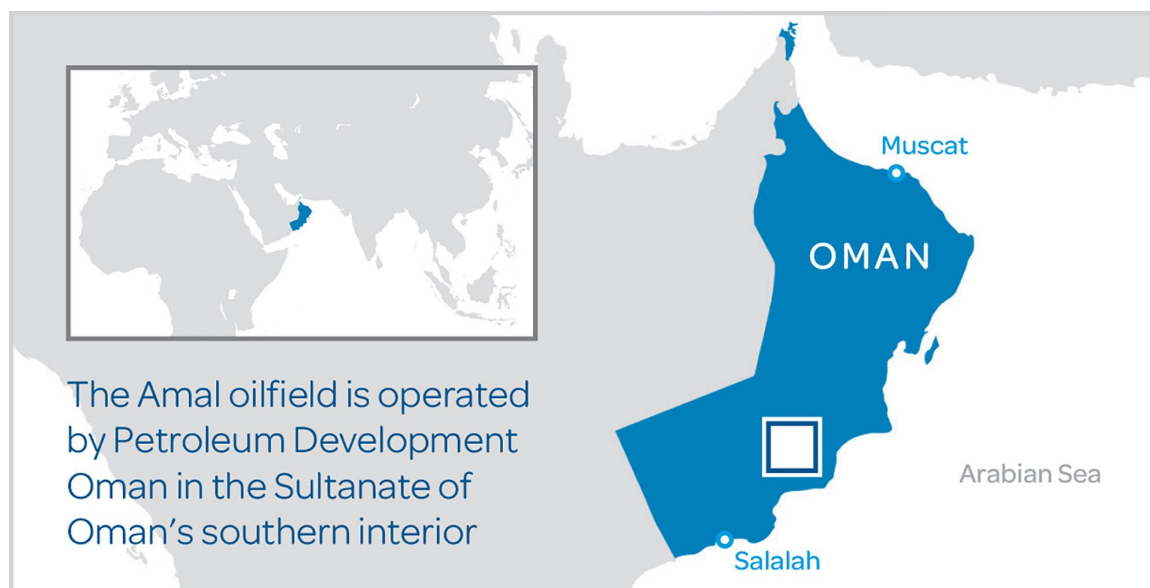


Figure 2. An illustrative map for Oman and the Amal oil field location (© GlassPoint, reproduced with permission).

Figure 3 illustrates the layout of the parabolic trough rows within an enclosing glasshouse [211]; the curved roof in the sketch corresponds to the Amal II pilot project. The looping of the heated water is noticeable in the sketch, where the heat addition process is cascaded through multiple passes along a sequence of trough rows.

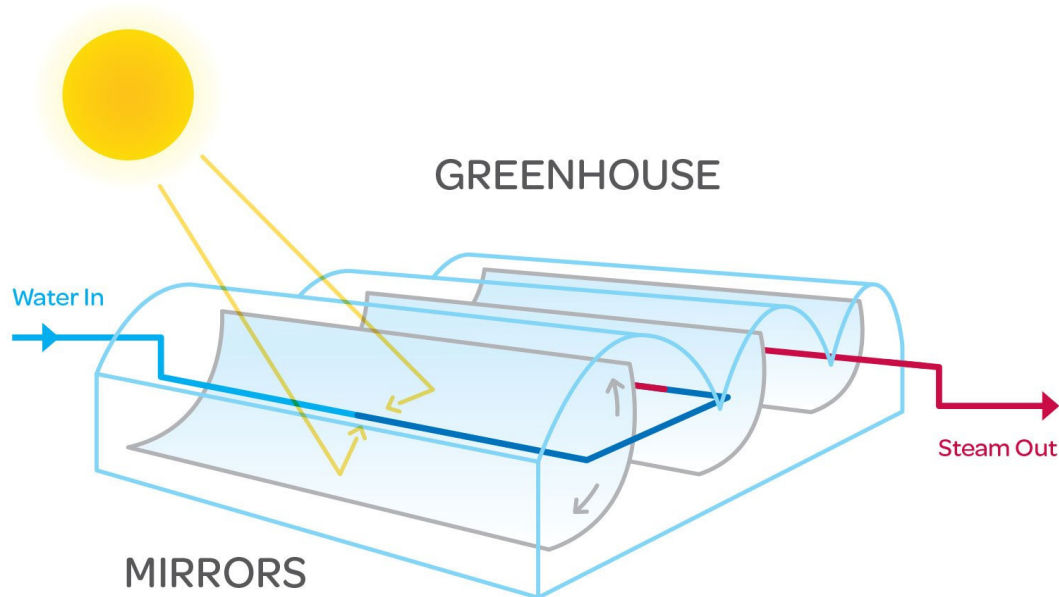


Figure 3. A sketch of the enclosed parabolic troughs and the water heating loop pipe (© GlassPoint, reproduced with permission).

Figure 4 further emphasizes the structural advantage behind the enclosure concept [212], where the fluid-structure interaction [213,214], as well as other environmental harsh influences such as dust and soiling effects, are prevented from affecting the parabolic reflector mirrors.

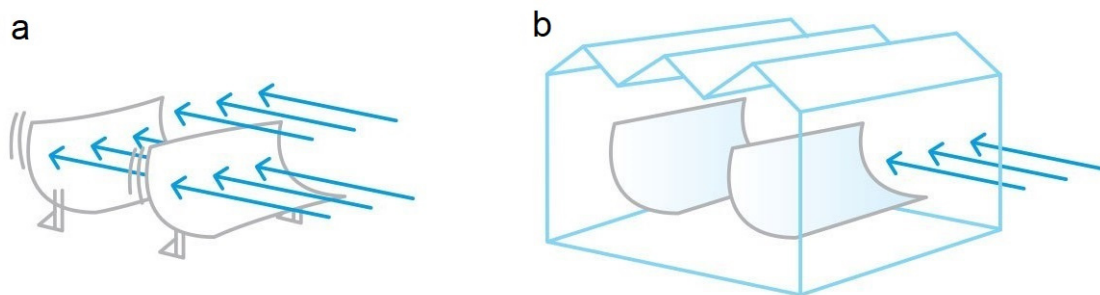


Figure 4. A sketch showing the wind load for (a) conventional (exposed) parabolic troughs, and (b) enclosed (protected) troughs (© GlassPoint, reproduced with permission).

Figure 5 visualizes the compactness advantage of the ESEOR concept as a source of energy [215] compared to the solar updraft tower (SUT) solar thermal technology [216,217], and the photovoltaic (PV) modules technology (the produced PV electricity should then be converted into heat using electric heaters) [218]. The close proximity of the trough rows in the ESEOR and the decreased soiling loss as a result of better automated daily cleaning make the design very efficient in terms of area utilization. In particular, the footprint demands of an SUT (solar tower) system are about 3 times those of the ESEOR system, while the footprint demands of a PV system are about 6 times those of the ESEOR system.

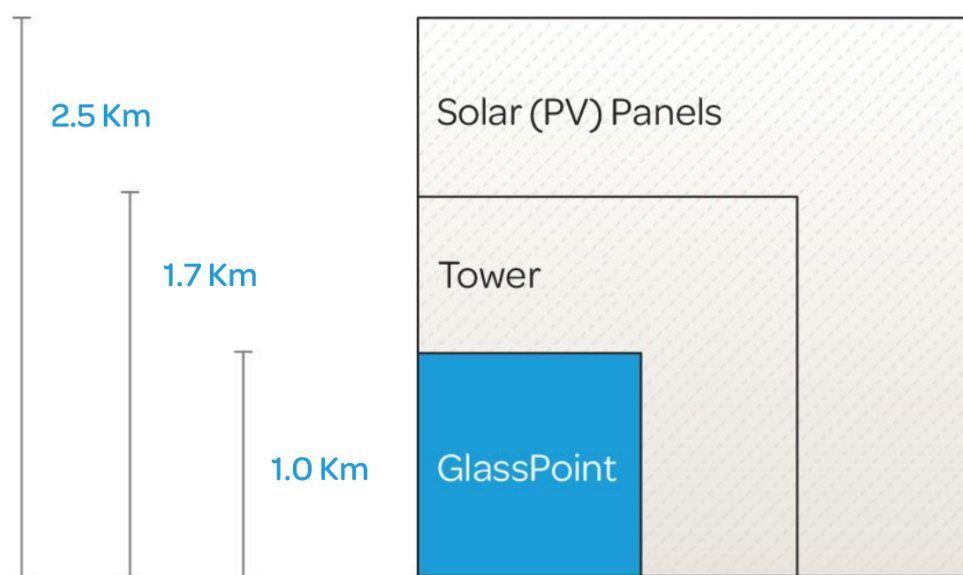


Figure 5. Comparison of the relative footprint area needs for different systems (© GlassPoint, reproduced with permission).

4.5. Selected Photos

It can be a valuable addition to the current study to show selected real photos that effectively describe the appearance of the three constructed ESEOR projects. This aim is fulfilled in the current subsection.

Figure 6 and Figure 7 are two photos taken for the Amal I pilot project [219,220]. The gable roof design is visible. The trough rows within the greenhouse-like enclosure show small spacing between rows as well as small tolerances at the two side tips of each row. Therefore, the ground coverage ratio (GCR) is close to one (around 0.93), which indicates a very compact design [221,222]. The ground coverage ratio (GCR) is the total mirror aperture surface area divided by the occupied ground area.

This high GCR contributes to the effective utilization of the land area. However, self-shading losses become high in the morning and the evening. It can also be noticed that the Amal I project has a single enclosure structure.

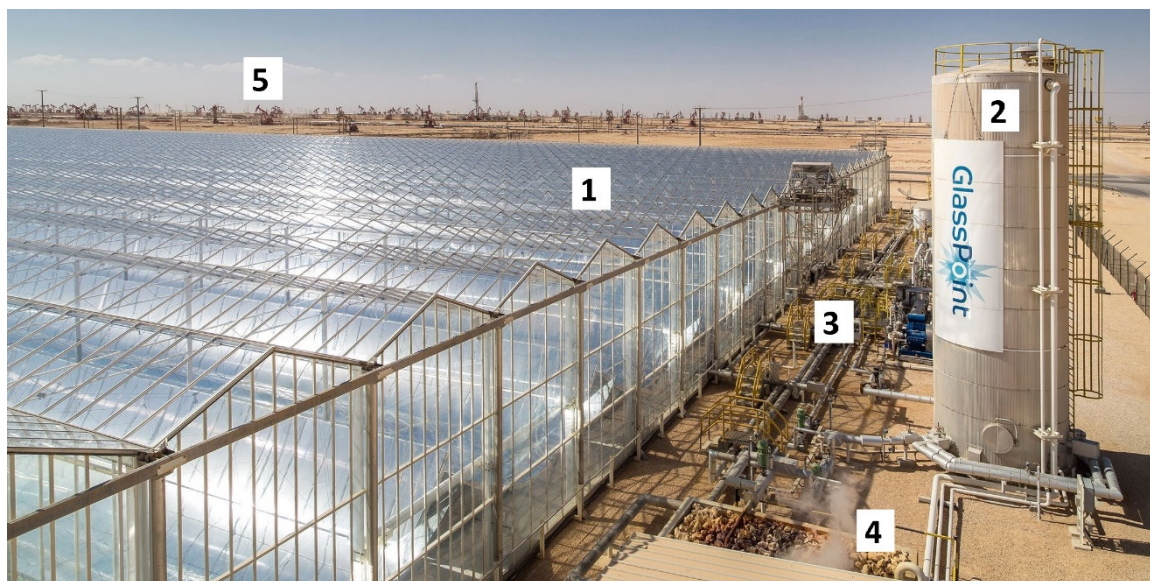


Figure 6. An aerial view of the Amal I pilot project (© GlassPoint, reproduced with permission). (1) Solar collector field, (2) Cylindrical water storage tank, (3) Steam distribution piping network, (4) Controlled steam vent (release point), (5) beam pumps (pump jacks) within the oil field.



Figure 7. A side photo of the Amal I pilot project (© GlassPoint, reproduced with permission).

Figure 8 is a photo taken for the Amal II pilot project [223]. The high ground coverage ratio (GCR) is apparent from this photo, as a result of small inter-row spacing and small tolerances between the rows and the adjacent enclosure walls. Like Amal I, the Amal II project consists of a single enclosure structure. The curved roof of Amal II is one of its main differences from Amal I.

Figure 9 is another photo of the Amal II pilot project during night installation, and it shows effectively one of the reflector mirrors and its supporting frame [224].



Figure 8. An aerial view of the Amal II pilot project (© GlassPoint, reproduced with permission). (1) Protective greenhouse enclosure, (2) Parabolic trough collector mirror, (3) Receiver pipe, (4) Beam pumps (pump jacks) within the oil field.

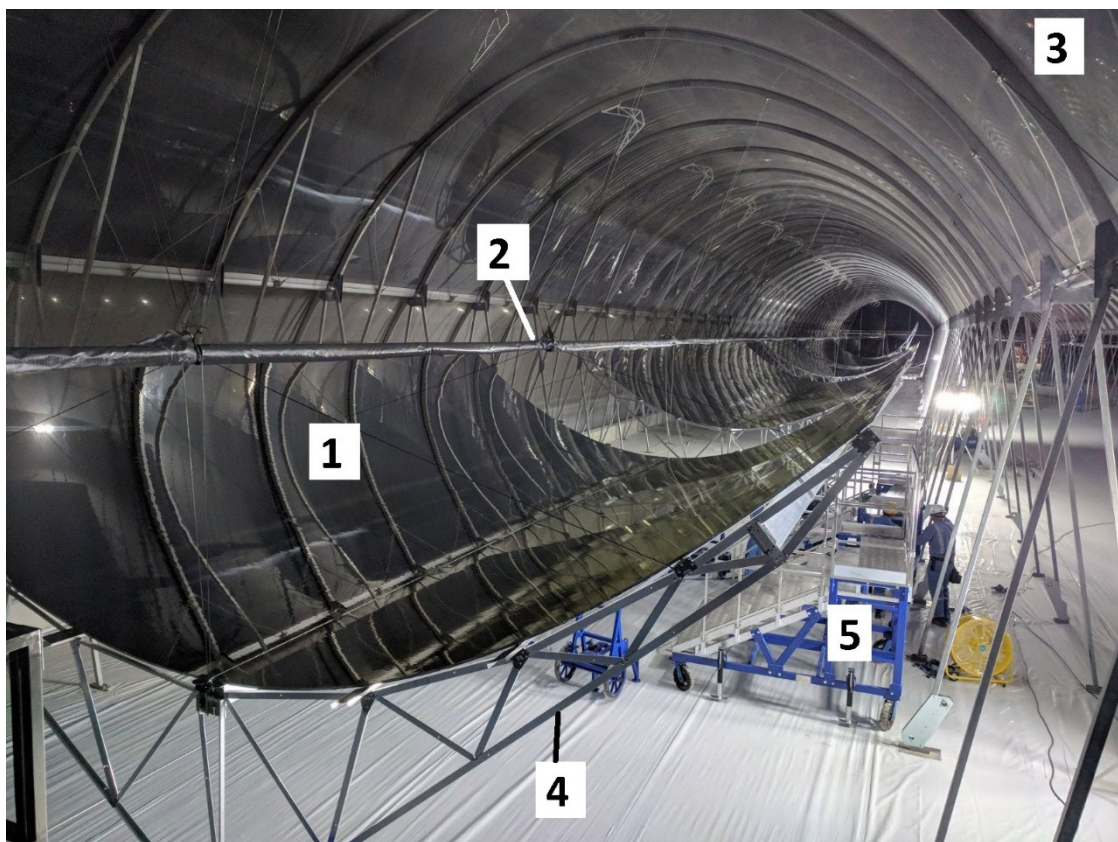


Figure 9. A photo showing night installation work at the Amal II pilot project (© GlassPoint, reproduced with permission). (1) Reflective collector surface, (2) Receiver pipe, (3) Roof of the protective enclosure, (4) Structural framework, (5) Installation equipment.

We visually illustrate the structure of the commercial-scale Miraah project. Given its larger scale compared to the pilot-scale Amal I and Amal II projects (the solar field area of Miraah is 36 times the solar field area of either Amal I or Amal II), the Miraah project is not constructed as a single enclosure. Instead, it is split over six enclosures and three modules. This is shown in Figure 10 [225].

Figure 11 is an on-site drone photo for one of the six enclosures of the Miraah project. A small portion of the adjacent enclosure can also be noticed [226]. The water/steam pipelines can be recognized well in this view.

Figure 12 is a front photo of one of the six enclosures of the Miraah project, showing the gable roof and outside pipelines [227]. The photo was taken near the solar noon (the sun is at its highest elevation), and therefore, the trough apertures are nearly pointing straight up. This particular view emphasizes the small clearance between the parabolic reflector mirrors. This maximizes the land utilization but at the expense of reduced capacity factor (CF) due to accentuated self-shading losses before and after the solar noon.

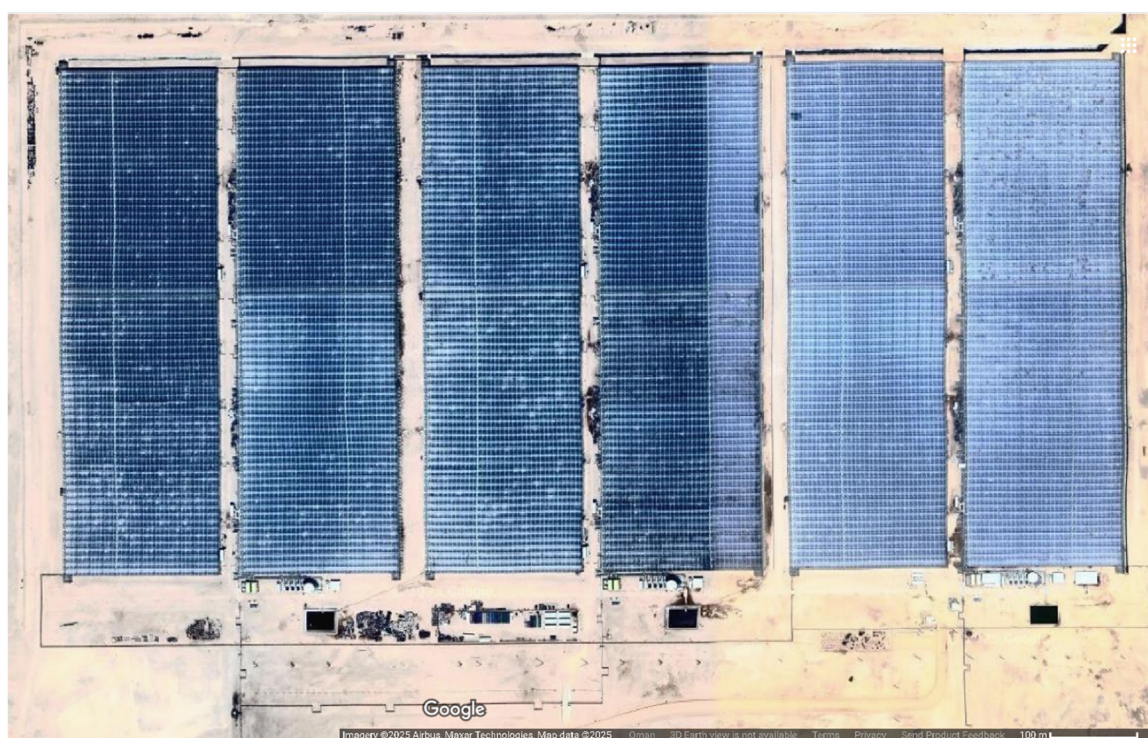


Figure 10. Satellite image of the Miraah commercial project, North is upward (© Google, Airbus, Maxar Technologies, Map data; permission granted under Google® Geo guidelines Database License [228]).



Figure 11. An aerial photo of one of the six zones of the Miraah commercial project (© GlassPoint, reproduced with permission). (1) Solar collector field (one of the six enclosures), (2) Steam distribution pipes, (3) Water storage tank, (4) Steam generation plant, (5) Control rooms/offices, (6) Pump skid (to pressurize liquid water and deliver it from the storage tank to the receiver tubes), (7) Water reservoir, (8) Adjacent solar collector enclosure.



Figure 12. A front photo of the Miraah commercial project (© GlassPoint, reproduced with permission). (1) Protective greenhouse enclosure, (2) Parabolic trough collector mirror, (3) Steam distribution pipe, (4) Electrical distribution panel.

4.6. Challenges

In this subsection, we discuss six challenges faced by the pioneering enclosed solar enhanced oil recovery (ESEOR) projects in Oman.

We compiled these challenges and the attempted mitigation actions and solutions from a variety of published works by GlassPoint staff as well as supplementary relevant external sources, as demonstrated by the cited reference(s) for each discussed challenge.

First, before even the installation phase, the large land area needed for an ESEOR project can be a challenge by itself. As in solar systems in general, the incoming solar radiation has relatively low density (around 1 kW/m^2 at its peak), and thus requires a large area to collect sufficiently useful heating rates [229–231]. A single receiver loop in the 54-loop Miraah project produces about 1.54 tonnes of steam per hour (about 13,500 tonnes of steam per annum), which requires heating freshwater at an intense rate of about 3.38 GJ/hour or 0.940 MWth. This is the bare minimum theoretical heating rate, without any losses. At peak operation, the realistic single-loop load jumps to 6.11 MWth or 22.0 GJ/hour. While this particular challenge was not problematic in the case of the Omani Amal oil field (due to the availability of unoccupied land), it might be a concern in another site.

Second, soiling in the open desert area of the Amal oil field can cause rapid loss of performance. While the transparent enclosure of the ESEOR protects the solar collector mirrors from dust and other soiling factors, the glass enclosure itself is subject to such soiling effects. This problem was addressed by daily night cleaning using a fast automatic roof washing (cleaning) system. The average soiling losses are kept at a maximum of 2% only between two consecutive daily washing processes. Due to dust infiltration, some internal soiling (inside the glasshouses) also occurs, but at a slow rate of about 0.2% per week. Due to the absence of condensation at the reflector mirrors, which is a condition attained by an air handling unit (AHU), dry, infrequent cloth-based cleaning is enough to restore the performance of the parabolic troughs and receiver tubes. A reverse osmosis (RO) plant is used to produce clean water for washing (cleaning) purposes that counteract soiling [185].

Third, due to having two sources of steam (the solar steam and the gas-firing steam) in the hybrid ESEOR projects in Oman, such hybrid steam generation systems require attention in terms of combining these two streams of steam. This was addressed by installing a production steam header, into which solar steam or gas-firing steam is injected directly. This header is charged at 88 bar to 100 bar [232].

Fourth, the weather at the Amal desert field can be very harsh, especially in the summer, when the ambient temperature approaches 50 °C at noon. This harmfully affects labor productivity as well as health and safety. This issue was mitigated by shifting the work from daytime to nighttime, where a drop of about 10 °C occurs [185].

Fifth, maintaining the receiver tube clear for the fluid flow requires special treatments. The water used at the Amal field is produced water (saline water separated from the extracted oil) [233], with about 8,000 ppm total dissolved solids (TDS) [234]. Such produced water is contaminated with dissolved minerals and probably with small solid particles. Therefore, it is important to prevent corrosion, erosion, and the deposition of solid matter on the internal walls of the receiver tube. These targets were achieved through multiple actions. Instead of the expensive demineralization treatment, water softening (as a limited but less expensive form of water treatment) was adopted, and water hardness was removed to less than 1 mg(CaCO₃)/L, which is very small [235,236]. Also, dissolved oxygen content is kept below 10 ppb using oxygen scavengers [237,238]. Accumulation of solid deposits is reduced by limiting the steam quality (steam dryness fraction) [239] at the boiler exit to 80%, which means that 20% (by mass) of this two-phase liquid-vapor water mixture is sufficient to dissolve soluble impurities. It should be noted that due to the variation of the solar irradiance during the day and the nonlinear heat transfer phenomena for solar heat generation [240,241], a control system [242] is installed to adjust the feedwater flow rate accordingly to maintain the target output steam quality [243–245]. Despite these preventive procedures, a small quantity of solids still inevitably accumulates in the receiver tubes. This is periodically removed through cleaning by hydraulically activated pipeline pigging (HAPP) [246]. The selection of carbon steel for the receiver tube was carefully made because of the high salt concentration of the feedwater. Alternative austenitic stainless alloys are not suitable here because they are susceptible to stress corrosion cracking (SCC) [247] upon exposure to chloride concentrations above 100 ppm [248,249].

Sixth, the limited capacity factor of an ESEOR project affects its economic feasibility. However, this low capacity factor can be increased if the rate of steam injection into the oil reservoir does not have to be at a constant rate during the 24-hour day. Instead, if more steam injection during the sunshine hours and less steam injection during the night are adopted, then the consumption of natural gas can be reduced further, to about 80%. This idea is possible because the heating and pressurization of the subsurface reservoir are not sensitive to the daily profile of steam injection. However, this idea implies elevated capital costs, increased operational maintenance costs, and added system complexity due to the oversized solar steam generation system. It also means that the oversized solar steam generation is more underutilized when the overall daily cycle is considered.

4.7. Steam-Oil Ratio (SOR)

In this subsection, we broadly discuss one of the key aspects of thermal enhanced oil recovery, which is the steam-oil ratio (SOR) [250], also called steam-to-oil ratio [251,252] and steam/oil ratio. This non-dimensional number is defined as the volume of water (converted into injected steam) to produce one volume of oil. The value of SOR can vary between two and eight [253]. In the case of the Omani solar enhanced oil recovery projects, a value of about three was reported. This is a favorable low value, reflecting an efficient use of steam. It is the same as the average steam-oil ratio (SOR) reported for the thermal enhanced oil recovery projects in Alberta, Canada [254]. The implication of the SOR is the water consumption for the thermal enhanced oil recovery. This consumption is aimed at being minimized for environmental and economic reasons. The profitability of steam-based EOR depends largely on the steam-oil ratio (SOR), due to affecting the operational cost [255]. It is worth mentioning that the steam-oil ratio might be reported in terms of the mass (kg steam/kg oil) [256] rather than the volume (m^3 steam/ m^3 oil).

5. Conclusions

We provided an overview of three novel sustainable enhanced oil recovery projects in Oman, in which clean steam produced by concentrated solar radiation partially replaces conventional steam produced by natural gas combustion, for the purpose of thermal enhanced oil recovery at the Amal oil field. Various design parameters, visualized structures, and challenges were discussed. This work is a case study that primarily aims to demonstrate and promote these successful examples for broader adoption in other geographic locations, which have large environmental gains.

We applied a thermal and emissions model to validate public data about the annual energy needs, annual natural gas consumption, and annual avoided carbon dioxide emissions. We found that the independently reported values are reasonably acceptable.

The current work did not cover the economic aspects of solar steam generation [257]. Also, some technological details were not mentioned here (such as the control system for steam injection, water storage, and automatic cleaning devices). Although these can be viewed as limitations, they help make the study focused and concise. These additional elements are valuable additions for coverage in a separate work.

The current work can be extended by examining thermal energy storage [258,259] as an added aspect in the Miraah solar enhanced oil recovery system. The technical gains from this idea can be assessed in terms of its ability to further reduce, or even eliminate, the demand for natural gas as a heating source at the Miraah project. This extension may require proper sizing of the storage capacity and exploring possible profiles of supplying steam to the reservoir (fixed rate versus variable rate).

For policymakers, the current study recommends expanded deployment of hybrid solar-steam generation systems for thermal enhanced oil recovery. The successful and endured operation of the Omani projects, as presented here, encourages governments and businesses to adopt this concept. The use of hybrid solar steam generation is not recommended only in enhanced oil recovery, but also in other processes that involve large heating demands. These include district heating [260,261], power generation [262–264], industrial drying [265], and food processing [266,267]. Governments can provide financial incentives [268–270] as well as technical awareness programs to motivate the transition toward this more sustainable heating alternative.

Funding: Not applicable (this research received no funding).

Data Availability Statement: The data that support the findings of this study are available within the article itself.

Declaration of Competing Interests Statement: The author declares that they have no known competing financial interests or personal relationships that could have appeared to influence the work reported in this paper.

References

- Williams, A. E. *Industrial Energy Systems Handbook*, 1st ed.; River Publishers: New York, USA, 2023. <https://doi.org/10.1201/9781003356431>.
- Lorenzini, G.; Moretti, S.; Conti, A. Units and Conversion Factors. In *Fin Shape Thermal Optimization Using Bejan's Constructal Theory*; Synthesis Lectures on Engineering; Springer International Publishing: Cham, Switzerland, 2011; pp 41–46. https://doi.org/10.1007/978-3-031-79333-2_5.
- NewMed Energy. *NewMed Energy / Energy Calculator*. <https://newmedenergy.com/energy-calculator/> (accessed 2025-08-02).
- Fanaritis, J. P.; Warren, Pa.; Kimmel, J. D. Review of Once-Through Steam Generators. *J Pet Technol* **1965**, *17* (04), 409–416. <https://doi.org/10.2118/1029-PA>.
- Tzanos, C. P. A Movable Boundary Model for Once-Through Steam Generator Analysis. *Nuclear Technology* **1988**, *82* (1), 5–17. <https://doi.org/10.13182/NT88-A34113>.
- YOON, J.; KIM, J.-P.; KIM, H.-Y.; LEE, D. J.; CHANG, M. H. Development of a Computer Code, ONCESG, for the Thermal-Hydraulic Design of a Once-Through Steam Generator. *Journal of Nuclear Science and Technology* **2000**, *37* (5), 445–454. <https://doi.org/10.1080/18811248.2000.9714917>.
- Lee, K. O.; Williams, W. C.; McFarlane, J.; Kropaczek, D.; de Wet, D. Semi-Empirical Model for Henry's Law Constant of Noble Gases in Molten Salts. *Sci Rep* **2024**, *14* (1), 12847. <https://doi.org/10.1038/s41598-024-60006-9>.
- Brown, N. L. *Renewable Energy Resources And Rural Applications In The Developing World*, 1st ed.; Routledge: New York, USA, 2019. <https://doi.org/10.4324/9780429304378>.
- EIA, [United States Energy Information Administration]. *EIA / Frequently Asked Questions (FAQs) = What are Ccf, Mcf, Btu, and therms?* <https://www.eia.gov/tools/faqs/faq.php?id=45&t=8> (accessed 2025-08-02).
- Khaledi, C. K. A.; Khosravi, M.; Tavousi, T.; Hamidianpour, M.; Moghadam, M. K. Future Warming of the Gulf of Oman: SST Trends under Contrasting Climate Scenarios by 2050. *Regional Studies in Marine Science* **2024**, *77*, 103682. <https://doi.org/10.1016/j.rsma.2024.103682>.
- World Bank. *CCKP / Climate Change Knowledge Portal - Oman (Historical Trends)*. <https://climateknowledgeportal.worldbank.org/country/oman/trends-variability-historical> (accessed 2025-06-07).
- Dreyfus, G. B.; Xu, Y.; Shindell, D. T.; Zaelke, D.; Ramanathan, V. Mitigating Climate Disruption in Time: A Self-Consistent Approach for Avoiding Both near-Term and Long-Term Global Warming. *Proceedings of the National Academy of Sciences* **2022**, *119* (22), e2123536119. <https://doi.org/10.1073/pnas.2123536119>.
- Marzouk, O. A.; Huckaby, E. D. Simulation of a Swirling Gas-Particle Flow Using Different k-Epsilon Models and Particle-Parcel Relationships. *Engineering Letters* **2010**, *18* (1).
- Pall, P.; Allen, M. R.; Stone, D. A. Testing the Clausius–Clapeyron Constraint on Changes in Extreme Precipitation under CO₂ Warming. *Clim Dyn* **2007**, *28* (4), 351–363. <https://doi.org/10.1007/s00382-006-0180-2>.
- Yamada, T. J.; Farukh, Murad. A.; Fukushima, T.; Inatsu, M.; Sato, T.; Pokhrel, Y. N.; Oki, T. Extreme Precipitation Intensity in Future Climates Associated with the Clausius-Clapeyron-like Relationship. *Hydrological Research Letters* **2014**, *8* (4), 108–113. <https://doi.org/10.3178/hrl.8.108>.
- Fowler, A. M.; Hennessy, K. J. Potential Impacts of Global Warming on the Frequency and Magnitude of Heavy Precipitation. *Nat Hazards* **1995**, *11* (3), 283–303. <https://doi.org/10.1007/BF00613411>.
- Huang, P.; Xie, S.-P.; Hu, K.; Huang, G.; Huang, R. Patterns of the Seasonal Response of Tropical Rainfall to Global Warming. *Nature Geosci* **2013**, *6* (5), 357–361. <https://doi.org/10.1038/ngeo1792>.
- Radwan, N.; Halder, B.; Ahmed, M. F.; Refadah, S. S.; Khan, M. Y. A.; Scholz, M.; Sammen, S. S.; Pande, C. B. Seasonal Precipitation and Anomaly Analysis in Middle East Asian Countries Using Google Earth Engine. *Water* **2025**, *17* (10), 1475. <https://doi.org/10.3390/w17101475>.
- Francis, D.; Fonseca, R.; Nelli, N.; Cherif, C.; Yarragunta, Y.; Zittis, G.; Jan de Vries, A. From Cause to Consequence: Examining the Historic April 2024 Rainstorm in the United Arab Emirates through the Lens of Climate Change. *npj Clim Atmos Sci* **2025**, *8* (1), 1–14. <https://doi.org/10.1038/s41612-025-01073-1>.
- GDACS, [Global Disaster Alert and Coordination System]. *Overall Green Alert Flood in Oman (GDACS ID: FL 1102566)*. <https://www.gdacs.org/report.aspx?eventtype=FL&eventid=1102566> (accessed 2025-05-25).

21. Marzouk, O. A. Assessment of Global Warming in Al Buraimi, Sultanate of Oman Based on Statistical Analysis of NASA POWER Data over 39 Years, and Testing the Reliability of NASA POWER against Meteorological Measurements. *Heliyon* **2021**, *7* (3), e06625. <https://doi.org/10.1016/j.heliyon.2021.e06625>.
22. Bruhwiler, L.; Basu, S.; Butler, J. H.; Chatterjee, A.; Dlugokencky, E.; Kenney, M. A.; McComiskey, A.; Montzka, S. A.; Stanitski, D. Observations of Greenhouse Gases as Climate Indicators. *Climatic Change* **2021**, *165* (1), 12. <https://doi.org/10.1007/s10584-021-03001-7>.
23. Marzouk, O. A. Temperature-Dependent Functions of the Electron–Neutral Momentum Transfer Collision Cross Sections of Selected Combustion Plasma Species. *Applied Sciences* **2023**, *13* (20), 11282. <https://doi.org/10.3390/app132011282>.
24. Szulejko, J. E.; Kumar, P.; Deep, A.; Kim, K.-H. Global Warming Projections to 2100 Using Simple CO₂ Greenhouse Gas Modeling and Comments on CO₂ Climate Sensitivity Factor. *Atmospheric Pollution Research* **2017**, *8* (1), 136–140. <https://doi.org/10.1016/j.apr.2016.08.002>.
25. Marzouk, O. A. Combined Oxy-Fuel Magnetohydrodynamic Power Cycle. In *Conference on Energy Challenges in Oman (ECO'2015)*; DU [Dhofar University]: Salalah, Dhofar, Oman, 2015.
26. Lindholt, L.; Glomsrød, S. Phasing out Coal and Phasing in Renewables – Good or Bad News for Arctic Gas Producers? *Energy Economics* **2018**, *70*, 1–11. <https://doi.org/10.1016/j.eneco.2017.12.015>.
27. Shindell, D.; Smith, C. J. Climate and Air-Quality Benefits of a Realistic Phase-out of Fossil Fuels. *Nature* **2019**, *573* (7774), 408–411. <https://doi.org/10.1038/s41586-019-1554-z>.
28. Marzouk, O. A. Recommended LEED-Compliant Cars, SUVs, Vans, Pickup Trucks, Station Wagons, and Two Seaters for Smart Cities Based on the Environmental Damage Index (EDX) and Green Score. In *Innovations in Smart Cities Applications Volume 7*; Ben Ahmed, M., Boudhir, A. A., El Meouche, R., Karaş, İ. R., Eds.; Lecture Notes in Networks and Systems; Springer Nature Switzerland: Cham, Switzerland, 2024; Vol. 906, pp 123–135. https://doi.org/10.1007/978-3-031-53824-7_12.
29. Nadimuthu, L. P. R.; Victor, K. Socio-Techno-Economic-Environmental Analysis of Vehicle-to-Grid-Integrated E-Mobility in Achieving Sustainable Development Goals: A Case Study. In *Handbook on New Paradigms in Smart Charging for E-Mobility*; Kumar, A., Bansal, R. C., Kumar, P., He, X., Eds.; Elsevier, 2025; pp 447–480. <https://doi.org/10.1016/B978-0-323-95201-9.00013-5>.
30. Marzouk, O. A. Urban Air Mobility and Flying Cars: Overview, Examples, Prospects, Drawbacks, and Solutions. *Open Engineering* **2022**, *12* (1), 662–679. <https://doi.org/10.1515/eng-2022-0379>.
31. Huang, A.; Dai, L.; Ali, S.; Nazar, R.; Anser, M. K. Zero-Emission Vision: The Role of E-Mobility Technology Budgets in Carbon Mitigation. *Transport Policy* **2025**, *164*, 265–280. <https://doi.org/10.1016/j.tranpol.2025.02.001>.
32. Vavouris, A.; Guasselli, F.; Stankovic, L.; Stankovic, V.; Gram-Hanssen, K.; Didierjean, S. A Complex Mixed-Methods Data-Driven Energy-Centric Evaluation of Net-Positive Households. *Applied Energy* **2024**, *367*, 123404. <https://doi.org/10.1016/j.apenergy.2024.123404>.
33. Zhu, Y.; Xu, W.; Luo, W.; Yang, M.; Chen, H.; Liu, Y. Application of Hybrid Machine Learning Algorithm in Multi-Objective Optimization of Green Building Energy Efficiency. *Energy* **2025**, *316*, 133581. <https://doi.org/10.1016/j.energy.2024.133581>.
34. Barhoumi, E. M.; Okonkwo, P. C.; Ben Belgacem, I.; Zghaibeh, M.; Tlili, I. Optimal Sizing of Photovoltaic Systems Based Green Hydrogen Refueling Stations Case Study Oman. *International Journal of Hydrogen Energy* **2022**, *47* (75), 31964–31973. <https://doi.org/10.1016/j.ijhydene.2022.07.140>.
35. Elkelawy, M.; Draz, A. M.; Antar, A. M.; Seleem, H. E. Enhancing Diesel Generator Efficiency and Emissions with CNG and Green Hydrogen: A Sustainable Solution for Power Plants. *Pharos Engineering Science Journal* **2025**. <https://doi.org/10.21608/pesj.2025.353885.1013>.
36. Squadrito, G.; Maggio, G.; Nicita, A. The Green Hydrogen Revolution. *Renewable Energy* **2023**, *216*, 119041. <https://doi.org/10.1016/j.renene.2023.119041>.
37. Marzouk, O. A. Levelized Cost of Green Hydrogen (LCOH) in the Sultanate of Oman Using H₂A-Lite with Polymer Electrolyte Membrane (PEM) Electrolyzers Powered by Solar Photovoltaic (PV) Electricity. *E3S Web of Conferences* **2023**, *469*, 00101. <https://doi.org/10.1051/e3sconf/202346900101>.

38. Mio, A.; Barbera, E.; Massi Pavan, A.; Bertuccio, A.; Fermeglia, M. Sustainability Analysis of Hydrogen Production Processes. *International Journal of Hydrogen Energy* **2024**, *54*, 540–553. <https://doi.org/10.1016/j.ijhydene.2023.06.122>.
39. Bauer, C.; Treyer, K.; Antonini, C.; Bergerson, J.; Gazzani, M.; Gencer, E.; Gibbins, J.; Mazzotti, M.; T. McCoy, S.; McKenna, R.; Pietzcker, R.; P. Ravikumar, A.; C. Romano, M.; Ueckerdt, F.; Vente, J.; Spek, M. van der. On the Climate Impacts of Blue Hydrogen Production. *Sustainable Energy & Fuels* **2022**, *6* (1), 66–75. <https://doi.org/10.1039/D1SE01508G>.
40. Marzouk, O. A. Detailed and Simplified Plasma Models in Combined-Cycle Magnetohydrodynamic Power Systems. *International Journal of Advanced and Applied Sciences* **2023**, *10* (11), 96–108. <https://doi.org/10.21833/ijaas.2023.11.013>.
41. Zhu, Q. *High-Efficiency Power Generation – Review of Alternative Systems*; IEA Clean Coal Cent: London, UK, 2015; pp 1–120. https://usea.org/sites/default/files/032015_High-efficiency%20power%20generation%20-%20review%20of%20alternative%20systems_ccc247.pdf (accessed 2025-05-26).
42. Marzouk, O. A. Detailed Derivation of the Scalar Explicit Expressions Governing the Electric Field, Current Density, and Volumetric Power Density in the Four Types of Linear Divergent MHD Channels Under a Unidirectional Applied Magnetic Field. *Contemporary Mathematics* **2025**, *6* (4), 4060–4100. <https://doi.org/10.37256/cm.6420256918>.
43. Marzouk, O. A.; Huckaby, E. D. New Weighted Sum of Gray Gases (WSGG) Models for Radiation Calculation in Carbon Capture Simulations: Evaluation and Different Implementation Techniques. In *7th U.S. National Technical Meeting of the Combustion Institute*; Atlanta, Georgia, USA, 2011; Vol. 4, pp 2483–2496.
44. Marzouk, O. A. Reduced-Order Modeling (ROM) of a Segmented Plug-Flow Reactor (PFR) for Hydrogen Separation in Integrated Gasification Combined Cycles (IGCC). *Processes* **2025**, *13* (5), 1455. <https://doi.org/10.3390/pr13051455>.
45. IEA, [International Energy Agency]. *IEA / World Energy Statistics and Balances*. IEA. <https://www.iea.org/data-and-statistics/data-product/world-energy-statistics-and-balances> (accessed 2025-07-31).
46. GEM, [Global Energy Monitor]. *Dhofar II Wind Farm - Global Energy Monitor Profile*. https://www.gem.wiki/Dhofar_II_wind_farm (accessed 2024-08-08).
47. MEM, [Minister of Energy and Minerals in the Sultanate of Oman]. *MEM / Dhofar wind farm*. <https://mem.gov.om/en-us/Our-Business/Renewable-Energy-and-Hydrogen/Renewable-Energy-and-Hydrogen-Projects/ArtMID/732/ArticleID/1325/Dhofar-wind-farm> (accessed 2024-10-28).
48. Masdar. *Dhofar Wind Power Project*; Public Announcement; 2022. https://masdar.ae/-/media/corporate/projects/downloads/dhofar-wind-power/dhofar-wind-power-project_eng.pdf (accessed 2023-10-30).
49. Marzouk, O. A. OpenFOAM Computational Fluid Dynamics (CFD) Solver for Magnetohydrodynamic Open Cycles, Applied to the Sakhalin Pulsed Magnetohydrodynamic Generator (PMHDG). *Discover Applied Sciences* **2025**, *7* (10), 1108. <https://doi.org/10.1007/s42452-025-07744-1>.
50. Marzouk, O. A. Changes in Fluctuation Waves in Coherent Airflow Structures with Input Perturbation. *WSEAS Transactions on Signal Processing* **2008**, *4* (10), 604–614.
51. York, R. How Much Can We Expect the Rise in U.S. Domestic Energy Production to Suppress Net Energy Imports? *Social Currents* **2015**. <https://doi.org/10.1177/2329496515589850>.
52. Rokicki, T.; Bórawski, P.; Szeberényi, A. The Impact of the 2020–2022 Crises on EU Countries' Independence from Energy Imports, Particularly from Russia. *Energies* **2023**, *16* (18), 6629. <https://doi.org/10.3390/en16186629>.
53. Yufenyuy, M.; Addai, K.; Kirikkaleli, D. Assessing the Effect of Transport Infrastructure Investments and Total Energy Supply on Material Footprint: Insights from France. *Energy & Environment* **2025**, 0958305X251326183. <https://doi.org/10.1177/0958305X251326183>.
54. Marzouk, O. A.; Huckaby, E. D. Assessment of Syngas Kinetic Models for the Prediction of a Turbulent Nonpremixed Flame. In *Fall Meeting of the Eastern States Section of the Combustion Institute*; College Park, Maryland, USA, 2009; pp 726–751.

55. Kazem, H. A. Renewable Energy in Oman: Status and Future Prospects. *Renewable and Sustainable Energy Reviews* **2011**, *15* (8), 3465–3469. <https://doi.org/10.1016/j.rser.2011.05.015>.
56. GEM, [Global Energy Monitor]. *GEM / Ibri 2 Solar - Profile*. https://www.gem.wiki/Ibri_2_Solar (accessed 2024-08-07).
57. MEM, [Sultanate of Oman Minister of Energy and Minerals]. *MEM / Ibri 2 Solar IPP*. <https://mem.gov.om/en-us/Our-Business/Renewable-Energy-and-Hydrogen/Renewable-Energy-and-Hydrogen-Projects/ArtMID/732/ArticleID/1324/Ibri-2-Solar-IPP> (accessed 2025-06-09).
58. MEM, [Ministry of Energy and Minerals in the Sultanate of Oman]. *MEM / The Sultanate of Oman's National Strategy for an Orderly Transition to Net Zero*; MEM [Ministry of Energy and Minerals in the Sultanate of Oman]: Muscat, Sultanate of Oman, 2022; pp 1–42. https://www.ea.gov.om/media/xdvpdu1w/oman-net-zero-report-2022_screen.pdf (accessed 2024-05-13).
59. Marzouk, O. A. University Role in Promoting Leadership and Commitment to the Community. In *Inaugural International Forum on World Universities*; Davos, Switzerland, 2008.
60. Al. Shibli, S. ICAO | Oman Vision 2040: A National Blueprint for Sustainable Environment and Clean Energy. In *ICAO 2025 Environmental Report - Skyward Action - Realizing Aviation's Sustainable Future*; ICAO [International Civil Aviation Organization]: Montreal, Canada, 2025; pp 257–259.
61. Marzouk, O. A. Benchmarking Retention, Progression, and Graduation Rates in Undergraduate Higher Education Across Different Time Windows. *Cogent Education* **2025**, *12* (1), 2498170. <https://doi.org/10.1080/2331186X.2025.2498170>.
62. OAAAQA, [Oman Authority for Academic Accreditation and Quality Assurance of Education]. *Institutional Standards Assessment Manual (ISAM) - Institutional Accreditation: Stage 2, Version 1*; Muscat, Sultanate of Oman, 2016. <https://oaaaqa.gov.om/getattachment/c63fde93-150b-430d-a58f-9f68e6dc2390/Institutional%20Standards%20Assessment%20Manual.aspx> (accessed 2024-10-08).
63. Marzouk, O. A. English Programs for Non-English Speaking College Students. In *1st Knowledge Globalization Conference 2008 (KGLOBAL 2008)*; Sawyer Business School, Suffolk University: Boston, Massachusetts, USA, 2008; pp 1–8.
64. OAAAQA, [Oman Authority for Academic Accreditation and Quality Assurance of Education]. *Programme Standards Assessment Manual (PSAM) - Programme Accreditation, Version 1*; Muscat, Sultanate of Oman, 2023. <https://oaaaqa.gov.om/getattachment/4359b83e-5ab9-4147-8e73-1ff0f9adcfce/Programme%20Standards%20Assessment%20Manual.aspx> (accessed 2024-10-08).
65. Marzouk, O. A. Benchmarking the Trends of Urbanization in the Gulf Cooperation Council: Outlook to 2050. In *1st National Symposium on Emerging Trends in Engineering and Management (NSETEM'2017)*; WCAS [Waljat College of Applied Sciences], Muscat, Oman, 2017; pp 1–9.
66. Om2040U, [Oman Vision 2040 Implementation Follow-up Unit]. *Oman Vision 2040 / Follow-up System*. <https://www.oman2040.om/organization?lang=en> (accessed 2024-07-30).
67. Om2040U, [Oman Vision 2040 Implementation Follow-up Unit]. *Oman 2040 Vision Document*; Om2040U [Oman Vision 2040 Implementation Follow-up Unit]: Muscat, Sultanate of Oman, 2020. <https://www.oman2040.om/VisionDocument?lang=en> (accessed 2023-10-06).
68. Om2040U, [Oman Vision 2040 Implementation Follow-up Unit]. *Oman Vision 2040 Implementation Follow-up Unit Website A Platform Promoting Transparency, Participation and Direct Communication*. <https://www.oman2040.om/news/6?lang=en> (accessed 2025-06-29).
69. Denney, D. EOR Potential in the Middle East: Current and Future Trends. *J Pet Technol* **2012**, *64* (01), 70–73. <https://doi.org/10.2118/0112-0070-JPT>.
70. Oxford Analytica. Oman Will Innovate to Meet Growing Energy Needs. *Expert Briefings* **2017**. <https://doi.org/10.1108/OXAN-DB220067>.
71. Nellist, M. D. Integration of Solar Steam Facilities with Existing Steam Generation Systems; OnePetro, 2018. <https://doi.org/10.2118/190441-MS>.
72. MacGregor, R. Q&A with Rod MacGregor, Chief Executive Officer and President, GlassPoint Solar. *J Pet Technol* **2013**, *65* (10), 62–63. <https://doi.org/10.2118/1013-0062-JPT>.
73. Shell. *Shell / Petroleum Development Oman (PDO)*. <https://www.shell.com.om/about-us/what-we-do/qalhat-Ing-saoc.html> (accessed 2025-06-28).

74. PDO, [Petroleum Development Oman]. *PDO / A Shining Beacon: Miraah Solar Project*. <https://www.pdo.co.om/en/Pages/Sustainability/EnvironmentalProjects.aspx?proID=3> (accessed 2025-08-02).
75. PDO, [Petroleum Development Oman]. *PDO / EcOman Centre*. <https://www.pdo.co.om/knowledge/world/Pages/ecoman.aspx> (accessed 2025-08-02).
76. GlassPoint. *GlassPoint / Press Release - MA'ADEN and GlassPoint sign a Memorandum of Understanding ("MOU") to develop the world's largest solar process steam plant*. GlassPoint. <https://www.glasspoint.com/maaden-press-release> (accessed 2025-08-25).
77. Sammy, T. D.; Ehirim, E. O.; Ugi, F. B. Modeling the Effect of Temperature for Enhanced Oil Recovery (EOR) Using Steam Injection Technique. *Journal of Newviews in Engineering and Technology* **2023**, 5 (1), 22–31.
78. Lee, K. S. The Effects of Temperature-Dependent Fluids Viscosity on the Performance of a Polymer Flood in Reservoir Systems with an Elevated Temperature. *Energy Sources, Part A: Recovery, Utilization, and Environmental Effects* **2011**, 33 (18), 1706–1714. <https://doi.org/10.1080/15567030903468544>.
79. Lee, K. S. Nonisothermal Assessment on the Performance of Polymer Flood in the Reservoir with Elevated Temperature; OnePetro, 2010. <https://doi.org/10.2118/132850-MS>.
80. Askarova, A.; Turakhanov, A.; Markovic, S.; Popov, E.; Maksakov, K.; Usachev, G.; Karpov, V.; Cheremisin, A. Thermal Enhanced Oil Recovery in Deep Heavy Oil Carbonates: Experimental and Numerical Study on a Hot Water Injection Performance. *Journal of Petroleum Science and Engineering* **2020**, 194, 107456. <https://doi.org/10.1016/j.petrol.2020.107456>.
81. Zhang, J. J. Chapter 2 - Rock Physical and Mechanical Properties. In *Applied Petroleum Geomechanics*; Zhang, J. J., Ed.; Gulf Professional Publishing, 2019; pp 29–83. <https://doi.org/10.1016/B978-0-12-814814-3.00002-2>.
82. Beyer, L. A.; Clutson, F. G. *USGS / Density and Porosity of Oil Reservoirs and Overlying Formations from Borehole Gravity Measurements, Gebo Oil Field, Hot Springs County, Wyoming*; USGS [United States Geological Survey], United States Department of the Interior: Reston, Virginia, USA, 1978; pp 1–24. <https://pubs.usgs.gov/of/088/report.pdf> (accessed 2025-08-02).
83. Sun, J.; Wang, B.; Shu, Y.; Wang, Y.; Pan, Y.; Tian, C. The Numerical Simulation Study on the Heat Transfer Mechanism in Heavy Oil Reservoirs During In-Situ Combustion. *Processes* **2025**, 13 (1), 56. <https://doi.org/10.3390/pr13010056>.
84. Sumeru, K.; Pramudiantoro, T. P.; Setyawan, A. Experimental Investigation on the Performance of Residential Air Conditioning System Using Water Condensate for Subcooling. *MATEC Web Conf.* **2018**, 197, 08002. <https://doi.org/10.1051/mateconf/201819708002>.
85. Tamainot-Telto, Z.; Metcalf, S. J.; Yande, N. N. Adsorption Solar Air Conditioning System for Singapore Climate. *Energies* **2022**, 15 (18), 6537. <https://doi.org/10.3390/en15186537>.
86. Kuma, Y.; Ozaki, A. Development of Central Air Conditioning Circulation System for Condominium Unit and Evaluation of the Indoor Environment in Summer. In *Advances in Computer Science and Ubiquitous Computing*; Park, J. S., Yang, L. T., Pan, Y., Park, J. J., Eds.; Springer Nature: Singapore, 2024; pp 49–55. https://doi.org/10.1007/978-981-97-2447-5_9.
87. Negara, I. G. A.; Temaja, I. W.; Midiani, L. P. I.; Santosa, I. D. M. C.; Wirajati, I. G. A. B.; Arsana, M. E. Experimental Analysis of Thermodynamic Performance for 2.5 kW Split Inverter Air Conditioning Unit with R-410A. *International Journal of Automotive and Mechanical Engineering* **2025**, 22 (2), 12388–12403. <https://doi.org/10.15282/ijame.22.2.2025.11.0948>.
88. Ross, S. A.; Cheah, L. Uncertainty Quantification in Life Cycle Assessments: Interindividual Variability and Sensitivity Analysis in LCA of Air-Conditioning Systems. *Journal of Industrial Ecology* **2017**, 21 (5), 1103–1114. <https://doi.org/10.1111/jiec.12505>.
89. Ahmad, A.; Prakash, O.; Kausher, R.; Kumar, G.; Pandey, S.; Hasnain, S. M. M. Parabolic Trough Solar Collectors: A Sustainable and Efficient Energy Source. *Materials Science for Energy Technologies* **2024**, 7, 99–106. <https://doi.org/10.1016/j.mset.2023.08.002>.
90. Bees Group. *Solar Heat for Industrial Process - SHIP*. <https://www.beesgroup.energy/en/services/solar-heat-for-industrial-process-ship> (accessed 2025-04-20).

91. EPA, [United States Environmental Protection Agency]. *Solar Heating and Cooling Technologies*. <https://19january2017snapshot.epa.gov/rhc/solar-heating-and-cooling-technologies> (accessed 2025-04-19).
92. Marzouk, O. A.; Al Kamzari, A. A.; Al-Hatmi, T. K.; Al Alawi, O. S.; Al-Zadjali, H. A.; Al Haseed, M. A.; Al Daqaq, K. H.; Al-Aliyani, A. R.; Al-Aliyani, A. N.; Al Balushi, A. A.; Al Shamsi, M. H. Energy Analyses for a Steam Power Plant Operating under the Rankine Cycle. In *First International Conference on Engineering, Applied Sciences and Management (UoB-IEASMA 2021)*; Al Kalbani, A. S., Kanna, R., EP Rabai, L. B., Ahmad, S., Valsala, S., Eds.; IEASMA Consultants LLP: Virtual, 2021; pp 11–22.
93. Perez Cordoba, J. H.; Gonzalez Sanchez, E. D.; Martinez Vertel, J. J.; Muñoz Navarro, S. F. Surface Facilities Development for Steam Flue Gas Injection in a Colombian Heavy Oil Reservoir; OnePetro, 2020. <https://doi.org/10.2118/199103-MS>.
94. Rodríguez, J. R.; Naranjo, P. A. L.; Molina, J. W.; Molina, J. D.; Molina, F.; Matute, A. K. Unveiling Success From Cyclic Steam Injections for Heavy Oil Recovery in India and the Orinoco Oil Belt; OnePetro, 2024. <https://doi.org/10.2118/218657-MS>.
95. Marzouk, O. A.; Jul, W. A. M. H. R.; Al Jabri, A. M. K.; Al-ghaithi, H. A. M. A. Construction of a Small-Scale Vacuum Generation System and Using It as an Educational Device to Demonstrate Features of the Vacuum. *International Journal of Contemporary Education* **2018**, *1* (2), 1–11. <https://doi.org/10.11114/ijce.v1i2.3554>.
96. Chien, S.-F. Empirical Correlations of Saturated Steam Properties. *SPE Res Eng* **1992**, *7* (02), 295–303. <https://doi.org/10.2118/20319-PA>.
97. Marzouk, O. A. A Two-Step Computational Aeroacoustics Method Applied to High-Speed Flows. *Noise Control Engineering Journal* **2008**, *56* (5), 396. <https://doi.org/10.3397/1.2978229>.
98. Egerton, A. C.; Callendar, G. S. On the Saturation Pressures of Steam (170° to 374° C.). *Philosophical Transactions of the Royal Society of London. Series A, Containing Papers of a Mathematical or Physical Character* **1997**, *231* (694–706), 147–205. <https://doi.org/10.1098/rsta.1933.0005>.
99. Struchtrup, H. *Thermodynamics and Energy Conversion*, 1st ed.; Springer-Verlag: Berlin, Germany, 2014.
100. ASME, [American Society of Mechanical Engineers]. *ASME Steam Tables, Compact Edition*; ASME [American Society of Mechanical Engineers]: New York City, New York, USA, 2007. <https://doi.org/10.1115/1.80254X>.
101. Verma, M. P. Steam Tables for Pure Water as an ActiveX Component in Visual Basic 6.0. *Computers & Geosciences* **2003**, *29* (9), 1155–1163. [https://doi.org/10.1016/S0098-3004\(03\)00136-5](https://doi.org/10.1016/S0098-3004(03)00136-5).
102. Marzouk, O. A. Thermo Physical Chemical Properties of Fluids Using the Free NIST Chemistry WebBook Database. *Fluid Mechanics Research International Journal* **2017**, *1* (1). <https://doi.org/10.15406/fmrij.2017.01.00003>.
103. Babita; Pant, U.; Meena, H.; Gupta, G.; Bapna, K.; Shivagan, D. D. Improved Realization of Ensemble of Triple Point of Water Cells at CSIR-NPL. *MAPAN* **2021**, *36* (3), 615–628. <https://doi.org/10.1007/s12647-021-00488-4>.
104. Wang, X.; Meijer, H. A. J. Ice–Liquid Isotope Fractionation Factors for ¹⁸O and ²H Deduced from the Isotopic Correction Constants for the Triple Point of Water. *Isotopes in Environmental and Health Studies* **2018**, *54* (3), 304–311. <https://doi.org/10.1080/10256016.2018.1435533>.
105. Hopwood, D. The New Hot Ticket [Concentrating Solar Thermal Power]. *Engineering & Technology* **2009**, *4* (15), 48–51. <https://doi.org/10.1049/et.2009.1507>.
106. Marzouk, O. A. A Flight-Mechanics Solver for Aircraft Inverse Simulations and Application to 3D Mirage-III Maneuver. *Global Journal of Control Engineering and Technology* **2015**, *1*, 14–26.
107. Núñez Bootello, J. P.; Mier-Torrecilla, M.; Doblaré, M.; Silva Pérez, M. Aerodynamics of New Solar Parametric Troughs: Two Dimensional and Three Dimensional Single Module Numerical Analysis. *Solar Energy* **2016**, *135*, 742–749. <https://doi.org/10.1016/j.solener.2016.06.040>.
108. Roschke, E. J. *Wind Loading on Solar Concentrators: Some General Considerations*; Contractor Report (CR) JPL-PUB-83-101; JPL [Jet Propulsion Laboratory]: Pasadena, California, USA, 1984; pp 1–174. <https://ntrs.nasa.gov/api/citations/19840024844/downloads/19840024844.pdf> (accessed 2025-08-02).
109. Marzouk, O. A. Contrasting the Cartesian and Polar Forms of the Shedding-Induced Force Vector in Response to 12 Subharmonic and Superharmonic Mechanical Excitations. *Fluid Dynamics Research* **2010**, *42* (3), 035507. <https://doi.org/10.1088/0169-5983/42/3/035507>.

110. Donaldson, E. C.; Chilingarian, G. V.; Yen, T. F. *Enhanced Oil Recovery, I: Fundamentals and Analyses*; Elsevier: Amsterdam, The Netherlands, 1985.
111. SLB, [Schlumberger Limited]. *SLB / Steam-Assisted Gravity Drainage*. https://glossary.slb.com/en/terms/s/steam-assisted_gravity_drainage (accessed 2025-10-31).
112. SLB, [Schlumberger Limited]. *SLB / Steamflood*. <https://glossary.slb.com/en/terms/s/steamflood> (accessed 2025-10-31).
113. SLB, [Schlumberger Limited]. *SLB / Huff and Puff*. https://glossary.slb.com/en/terms/h/huff_and_puff (accessed 2025-10-31).
114. SLB, [Schlumberger Limited]. *SLB / Cyclic Steam Injection*. https://glossary.slb.com/en/terms/c/cyclic_steam_injection (accessed 2025-10-31).
115. Johns, R. T. Oil Recovery. In *Encyclopedia of Energy*; Cleveland, C. J., Ed.; Elsevier: New York, 2004; pp 701–713. <https://doi.org/10.1016/B0-12-176480-X/00255-2>.
116. Bera, A.; Vij, R. K.; Shah, S. Impact of Newly Implemented Enhanced Oil and Gas Recovery Screening Policy on Current Oil Production and Future Energy Supply in India. *Journal of Petroleum Science and Engineering* **2021**, *207*, 109196. <https://doi.org/10.1016/j.petrol.2021.109196>.
117. DOE, [United States Department of Energy]. *DOE / Enhanced Oil Recovery*. <https://www.energy.gov/fecm/enhanced-oil-recovery> (accessed 2025-10-31).
118. SLB, [Schlumberger Limited]. *SLB / Miscible Displacement*. https://glossary.slb.com/en/terms/m/miscible_displacement (accessed 2025-10-31).
119. Kalita, P.; Sharma, V.; Pandey, L.; Tiwari, P. Secondary and Tertiary Oil Recovery Processes. In *Microbial Enhanced Oil Recovery: Principles and Potential*; Pandey, L., Tiwari, P., Eds.; Springer: Singapore, 2022; pp 23–50. https://doi.org/10.1007/978-981-16-5465-7_2.
120. Wang, Y.; Zhang, L.; Zhao, Y.; Zhou, X.; Lu, S.; Zhang, D.; Qin, J.; Lei, Z.; Tian, Y. Novel Approach to Enhancing Tight Oil Recovery Using N₂-Assisted CO₂ Flooding and Its Potential for CO₂ Storage. *Energy Fuels* **2023**, *37* (11), 7667–7678. <https://doi.org/10.1021/acs.energyfuels.3c00312>.
121. SLB, [Schlumberger Limited]. *SLB / Secondary Recovery*. https://glossary.slb.com/terms/s/secondary_recovery (accessed 2025-10-31).
122. Mohan, K.; Gupta, R.; Mohanty, K. K. Wettability Altering Secondary Oil Recovery in Carbonate Rocks. *Energy Fuels* **2011**, *25* (9), 3966–3973. <https://doi.org/10.1021/ef200449y>.
123. SLB, [Schlumberger Limited]. *SLB / Primary Recovery*. https://glossary.slb.com/en/terms/p/primary_recovery (accessed 2025-10-31).
124. Solaimany-Nazar, A. R.; Zonnouri, A. Modeling of Asphaltene Deposition in Oil Reservoirs during Primary Oil Recovery. *Journal of Petroleum Science and Engineering* **2011**, *75* (3), 251–259. <https://doi.org/10.1016/j.petrol.2010.11.017>.
125. Hoy, M.; Derler, M.; Lobianco, L.; Knauhs, P.; Marschall, C. Artificial Lift Failures and Operational Challenges in a Chemical EOR Field - A Comparative Analysis of Sucker Rod Pumps and Electric Submersible Pumps; OnePetro, 2024. <https://doi.org/10.2118/221503-MS>.
126. SLB, [Schlumberger Limited]. *SLB / Artificial Lift*. https://glossary.slb.com/en/terms/a/artificial_lift (accessed 2025-10-31).
127. SLB, [Schlumberger Limited]. *SLB / Gas Lift*. https://glossary.slb.com/en/terms/g/gas_lift (accessed 2025-10-31).
128. Mokheimer, E. M. A.; Hamdy, M.; Abubakar, Z.; Shakeel, M. R.; Habib, M. A.; Mahmoud, M. A. Comprehensive Review of Thermal Enhanced Oil Recovery: Techniques Evaluation. *Journal of Energy Resources Technology* **2018**, *141* (030801). <https://doi.org/10.1115/1.4041096>.
129. Parshall, J. Challenges, Opportunities Abound for Artificial Lift. *J Pet Technol* **2013**, *65* (03), 70–75. <https://doi.org/10.2118/0313-0070-JPT>.
130. Bucaram, S. M. Managing Artificial Lift. *J Pet Technol* **1994**, *46* (04), 335–340. <https://doi.org/10.2118/26212-PA>.
131. von Flatern, R. Artificial Lift. *Oilfield Review* **2015**, *27* (2), 1–2.
132. Mahdi, M. A. A.; Amish, M.; Oluyemi, G. An Artificial Lift Selection Approach Using Machine Learning: A Case Study in Sudan. *Energies* **2023**, *16* (6), 2853. <https://doi.org/10.3390/en16062853>.

133. SLB, [Schlumberger Limited]. *SLB / Injection Well*. https://glossary.slb.com/en/terms/i/injection_well (accessed 2025-10-31).
134. SLB, [Schlumberger Limited]. *SLB / Gas Cap*. https://glossary.slb.com/en/terms/g/gas_cap (accessed 2025-10-31).
135. SLB, [Schlumberger Limited]. *SLB / Gas Injection*. https://glossary.slb.com/en/terms/g/gas_injection (accessed 2025-10-31).
136. Khan, W. A.; Rui, Z.; Hu, T.; Liu, Y.; Zhang, F.; Zhao, Y. Application of Machine Learning and Optimization of Oil Recovery and CO₂ Sequestration in the Tight Oil Reservoir. *SPE J.* **2024**, *29* (06), 2772–2792. <https://doi.org/10.2118/219731-PA>.
137. Yu, G.; Xu, F.; Cui, Y.; Li, X.; Kang, C.; Lu, C.; Li, S.; Bai, L.; Du, S. A New Method of Predicting the Saturation Pressure of Oil Reservoir and Its Application. *International Journal of Hydrogen Energy* **2020**, *45* (55), 30244–30253. <https://doi.org/10.1016/j.ijhydene.2020.08.042>.
138. Smith, D. D.; Ambastha, A.; Ayirala, S.; Bai, B.; Carreras, P.; Hampton, D.; Mohanty, K.; Rossen, W.; Schoeling, L.; Yousef, A. *IOR and EOR Terminology Clarifications and Recommendations for the SPE Community*; Society of Petroleum Engineers, 2024. <https://doi.org/10.2118/223930-TR>.
139. Shakeel, M.; Sagandykova, D.; Mukhtarov, A.; Dauyltayeva, A.; Maratbekkyzy, L.; Pourafshary, P.; Musharova, D. Maximizing Oil Recovery: Innovative Chemical EOR Solutions for Residual Oil Mobilization in Kazakhstan's Waterflooded Sandstone Oilfield. *Heliyon* **2024**, *10* (7). <https://doi.org/10.1016/j.heliyon.2024.e28915>.
140. Thomas, S. Enhanced Oil Recovery - An Overview. *Oil & Gas Science and Technology - Rev. IFP* **2008**, *63* (1), 9–19. <https://doi.org/10.2516/ogst.2007060>.
141. Tirado, A.; Félix, G.; Trejo, F.; Varfolomeev, M. A.; Yuan, C.; Nurgaliev, D. K.; Sámano, V.; Ancheyta, J. Properties of Heavy and Extra-Heavy Crude Oils. In *Catalytic In-Situ Upgrading of Heavy and Extra-Heavy Crude Oils*; John Wiley & Sons, Ltd., 2023; pp 1–38. <https://doi.org/10.1002/9781119871507.ch1>.
142. Huc, A.-Y. *Heavy Crude Oils: From Geology to Upgrading : An Overview*; Editions TECHNIP, 2011.
143. El Bassoussi, A. A.; El-sabagh, S. M.; Harb, F. M.; El Nady, M. M. Characterization and Correlation of Crude Oils from Some Wells in the North Western Desert, Egypt. *Petroleum Science and Technology* **2018**, *36* (5), 384–391. <https://doi.org/10.1080/10916466.2018.1427107>.
144. Alizadeh, S.; Ta, S.; Ray, A. K.; Lakshminarayanan, S. Determination of Density and Viscosity of Crude Oil Samples from FTIR Data Using Multivariate Regression, Variable Selection and Classification. *IFAC-PapersOnLine* **2022**, *55* (7), 845–850. <https://doi.org/10.1016/j.ifacol.2022.07.550>.
145. Correa Pabón, R. E.; Souza Filho, C. R. de. Crude Oil Spectral Signatures and Empirical Models to Derive API Gravity. *Fuel* **2019**, *237*, 1119–1131. <https://doi.org/10.1016/j.fuel.2018.09.098>.
146. Lammoglia, T.; Filho, C. R. de S. SATELLITE DETERMINATION OF API GRAVITY AND SARA COMPONENTS OF OFFSHORE PETROLEUM SEEPS. *Brazilian Journal of Geophysics* **2012**, *30* (4), 419–430. <https://doi.org/10.22564/rbgf.v30i4.229>.
147. Zuo, J. Y.; Mullins, O. C.; Freed, D.; Zhang, D. A Simple Relation between Solubility Parameters and Densities for Live Reservoir Fluids. *J. Chem. Eng. Data* **2010**, *55* (9), 2964–2969. <https://doi.org/10.1021/je100155d>.
148. Farkha, S. A.; Zangana, M. H. S.; Shoham, O. Evaluation of Compositional Models and PVT Correlations for Iraqi Light Crude Oils Properties. *Energy Science & Engineering* **2023**, *11* (7), 2654–2667. <https://doi.org/10.1002/ese3.1456>.
149. Poirier, L.; Nelson, J.; Leong, D.; Berhane, L.; Hajdu, P.; Lopez-Linares, F. Application of ICP-MS and ICP-OES on the Determination of Nickel, Vanadium, Iron, and Calcium in Petroleum Crude Oils via Direct Dilution. *Energy Fuels* **2016**, *30* (5), 3783–3790. <https://doi.org/10.1021/acs.energyfuels.5b02997>.
150. *Solar Thermal Conversion Technologies for Industrial Process Heating*, 1st ed.; Arjunan, T. V., Selvaraj, V., Matheswaran, M. M., Eds.; CRC Press: Boca Raton, Florida, USA, 2023. <https://doi.org/10.1201/9781003263326>.
151. GlassPoint. *GlassPoint projects*. <https://www.glasspoint.com/projects> (accessed 2025-05-24).
152. GlassPoint. *GlassPoint technology*. <https://www.glasspoint.com/technology> (accessed 2025-05-24).

153. SHC, [Solar Heating and Cooling Programme]. *Solar Heat for Industrial Processes (SHIP)*; Technology Position Paper; IEA [International Energy Agency]: Paris, France, 2024; pp 1–9. <https://www.iea-shc.org/Data/Sites/1/publications/IEA-SHC-Task64-Technology-Position-Paper-SHIP-2024-01.pdf> (accessed 2025-04-18).
154. Kalogirou, S. A. Solar Thermal Collectors and Applications. *Progress in Energy and Combustion Science* **2004**, *30* (3), 231–295. <https://doi.org/10.1016/j.pecs.2004.02.001>.
155. Barone, G.; Buonomano, A.; Forzano, C.; Palombo, A. Chapter 6 - Solar Thermal Collectors. In *Solar Hydrogen Production*; Calise, F., D'Accadia, M. D., Santarelli, M., Lanzini, A., Ferrero, D., Eds.; Academic Press, 2019; pp 151–178. <https://doi.org/10.1016/B978-0-12-814853-2.00006-0>.
156. Goswami, D. Y. *Principles of Solar Engineering*, 4th ed.; CRC Press: Boca Raton, Florida, USA, 2022. <https://doi.org/10.1201/9781003244387>.
157. Sheikholeslami, M. *Solar Thermal Systems and Applications: New Design Techniques for Improved Thermal Performance*; Elsevier: London, UK, 2024.
158. ASI, [Atlantica Sustainable Infrastructure Ltd.]. *ASI / Powering the energy transition - Mojave*. <https://atlantica.com/business/assets/asset/mojave/> (accessed 2025-11-01).
159. CEC, [California Energy. CEC / Mojave Solar Project (Abengoa)]. <https://www.energy.ca.gov/powerplant/solar-thermal/mojave-solar-project-abengoa> (accessed 2025-11-01).
160. Gallego, A. J.; Macías, M.; de Castilla, F.; Camacho, E. F. Mathematical Modeling of the Mojave Solar Plants. *Energies* **2019**, *12* (21), 4197. <https://doi.org/10.3390/en12214197>.
161. Tagle-Salazar, P. D.; Nigam, K. D. P.; Rivera-Solorio, C. I. Parabolic Trough Solar Collectors: A General Overview of Technology, Industrial Applications, Energy Market, Modeling, and Standards. *Green Processing and Synthesis* **2020**, *9* (1), 595–649. <https://doi.org/10.1515/gps-2020-0059>.
162. Fernández-García, A.; Zarza, E.; Valenzuela, L.; Pérez, M. Parabolic-Trough Solar Collectors and Their Applications. *Renewable and Sustainable Energy Reviews* **2010**, *14* (7), 1695–1721. <https://doi.org/10.1016/j.rser.2010.03.012>.
163. Paetzold, J.; Cochard, S.; Fletcher, D. F.; Vassallo, A. Wind Engineering Analysis of Parabolic Trough Collectors to Optimise Wind Loads and Heat Loss. *Energy Procedia* **2015**, *69*, 168–177. <https://doi.org/10.1016/j.egypro.2015.03.020>.
164. NREL, [United States National Renewable Energy Laboratory]. *NREL / Parabolic Trough Solar Thermal Electric Power Plants*; NREL [United States National Renewable Energy Laboratory], 2006. <https://docs.nrel.gov/docs/fy06osti/40211.pdf> (accessed 2025-11-01).
165. Mishra, S. *Solar Square / Parabolic Trough Collector: Working, Benefits, And Drawbacks*. Rooftop Solar for your home and more - Blog | SolarSquare. <https://solarsquare.in/blog/parabolic-trough-collector/> (accessed 2025-11-01).
166. Natraj; Rao, B. N.; Reddy, K. S. Wind Load and Structural Analysis for Standalone Solar Parabolic Trough Collector. *Renewable Energy* **2021**, *173*, 688–703. <https://doi.org/10.1016/j.renene.2021.04.007>.
167. Marzouk, O. A.; Nayfeh, A. H. Simulation, Analysis, and Explanation of the Lift Suppression and Break of 2:1 Force Coupling Due to in-Line Structural Vibration. In *49th AIAA/ASME/ASCE/AHS/ASC Structures, Structural Dynamics, and Materials Conference*; AIAA [American Institute of Aeronautics and Astronautics]: Schaumburg, Illinois, USA, 2008; p AIAA 2008-2309. <https://doi.org/10.2514/6.2008-2309>.
168. Marzouk, O. A. Directivity and Noise Propagation for Supersonic Free Jets. In *46th AIAA Aerospace Sciences Meeting and Exhibit*; AIAA [American Institute of Aeronautics and Astronautics]: Reno, Nevada, USA, 2008; p AIAA 2008-23. <https://doi.org/10.2514/6.2008-23>.
169. Marzouk, O. A. Accurate Prediction of Noise Generation and Propagation. In *18th Engineering Mechanics Division Conference of the American Society of Civil Engineers (ASCE-EMD)*; Zenodo: Blacksburg, Virginia, USA, 2007; pp 1–6.
170. Marzouk, O. A. Solar Heat for Industrial Processes (SHIP): An Overview of Its Categories and a Review of Its Recent Progress. *Solar* **2025**, *5* (4), 46. <https://doi.org/10.3390/solar5040046>.
171. GlassPoint. *GlassPoint / Maaden Solar I*. <https://www.glasspoint.com/projects/maaden-solar> (accessed 2025-08-11).

172. Kar, M. K.; Önal, M. A. R.; Borra, C. R. Alumina Recovery from Bauxite Residue: A Concise Review. *Resources, Conservation and Recycling* **2023**, *198*, 107158. <https://doi.org/10.1016/j.resconrec.2023.107158>.
173. Donoghue, A. M.; Frisch, N.; Olney, D. Bauxite Mining and Alumina Refining: Process Description and Occupational Health Risks. *Journal of Occupational and Environmental Medicine* **2014**, *56*, S12. <https://doi.org/10.1097/JOM.0000000000000001>.
174. Waghmare, S. A.; Gulhane, N. P. Optical Evaluation of Compound Parabolic Collector with Low Acceptance Angle. *Optik* **2017**, *149*, 359–371. <https://doi.org/10.1016/j.ijleo.2017.09.039>.
175. Schizas, C. N.; Kalogirou, S.; Neocleous, C. A Comparative Study of Methods for Estimating Intercept Factor of Parabolic Trough Collectors. In *Engineering Applications of Neural Networks Conference*; London, UK, 1996.
176. Christian, J. M.; Ho, C. K. Finite Element Modeling and Ray Tracing of Parabolic Trough Collectors for Evaluation of Optical Intercept Factors With Gravity Loading; American Society of Mechanical Engineers Digital Collection, 2012; pp 577–585. <https://doi.org/10.1115/ES2011-54238>.
177. Kosić, T.; Svetel, I. Technological and Economical Analysis of Curved Glass Structure. *Structural Integrity and Life* **2022**, *22* (2), 175–181.
178. Louter, C.; Bos, F.; Belis, J.; Lebet, J.-P. *Challenging Glass 4 & COST Action TU0905 Final Conference*; CRC Press: Boca Raton, Florida, USA, 2014.
179. Li, J.; Wang, Z.; Li, J.; Lei, D. Vacuum Reliability Analysis of Parabolic Trough Receiver. *Solar Energy Materials and Solar Cells* **2012**, *105*, 302–308. <https://doi.org/10.1016/j.solmat.2012.06.034>.
180. Pourbafrani, M.; Ghadamian, H.; Aminy, M.; Moghadasi, M.; Mardani, M.; Akrami, M.; Khaki, A. H.; Sadr, S. M. K. Improving the Energy Performance of an Evacuated Tube Solar Collector Water Heater Using Compound Parabolic Concentrator: An Experimental Study. *Journal of Renewable Energy and Environment* **2024**, *11* (2), 58–66. <https://doi.org/10.30501/jree.2024.424000.1728>.
181. Bierman, B.; Treynor, C.; O'Donnell, J.; Lawrence, M.; Chandra, M.; Farver, A.; Von Behrens, P.; Lindsay, W. Performance of an Enclosed Trough EOR System in South Oman. *Energy Procedia* **2014**, *49*, 1269–1278. <https://doi.org/10.1016/j.egypro.2014.03.136>.
182. GlassPoint. *Amal I project in Oman*. <https://www.glasspoint.com/projects/amal> (accessed 2025-05-24).
183. Wilson, A. Pilot Steam Generator Uses Solar Energy Successfully for EOR Operations in Oman. *J Pet Technol* **2015**, *67* (06), 111–113. <https://doi.org/10.2118/0615-0111-JPT>.
184. GlassPoint. *Amal II project in Oman*. <https://www.glasspoint.com/projects/amal2> (accessed 2025-05-24).
185. Bierman, B.; Al-Lawatia, H.; DiFilippo, M.; O'Donnell, J. Deploying Enclosed Trough for Thermal EOR at Commercial Scale. *AIP Conference Proceedings* **2018**, *2033* (1), 030002. <https://doi.org/10.1063/1.5067018>.
186. GlassPoint. *Miraah project in Oman*. <https://www.glasspoint.com/projects/miraah> (accessed 2025-05-24).
187. Madaeni, S. H.; Sioshansi, R.; Denholm, P. Estimating the Capacity Value of Concentrating Solar Power Plants With Thermal Energy Storage: A Case Study of the Southwestern United States. *IEEE Transactions on Power Systems* **2013**, *28* (2), 1205–1215. <https://doi.org/10.1109/TPWRS.2012.2207410>.
188. Falahati, B.; Kargarian, A.; Fu, Y. Timeframe Capacity Factor Reliability Model for Isolated Microgrids with Renewable Energy Resources. In *2012 IEEE Power and Energy Society General Meeting*; 2012; pp 1–8. <https://doi.org/10.1109/PESGM.2012.6345546>.
189. Kamnappure, N. R.; Reddy, K. S. Optical Analysis of Solar Parabolic Trough Collector with Flat Concentrating Photovoltaic Receiver. *Applied Mechanics and Materials* **2014**, *592–594*, 2396–2403. <https://doi.org/10.4028/www.scientific.net/AMM.592-594.2396>.
190. Giovannetti, F.; Horta, P. *IEA SHC / Comparison of Process Heat Collectors with Respect to Technical and Economic Conditions*; Technical Report A.2.1; IEA SHC [International Energy Agency - Solar Heating and Cooling Programme]; Paris, France, 2016; pp 1–36. [https://w.iea-shc.org/Data/Sites/1/publications/Task%2049%20Deliverable%20A2%201_End%20\(3\).pdf](https://w.iea-shc.org/Data/Sites/1/publications/Task%2049%20Deliverable%20A2%201_End%20(3).pdf) (accessed 2025-08-02).
191. Quaschnig, V.; Kistner, R.; Ortmanns, W. Influence of Direct Normal Irradiance Variation on the Optimal Parabolic Trough Field Size: A Problem Solved with Technical and Economical Simulations. *J. Sol. Energy Eng* **2002**, *124* (2), 160–164. <https://doi.org/10.1115/1.1465432>.

192. Blanc, P.; Espinar, B.; Geuder, N.; Gueymard, C.; Meyer, R.; Pitz-Paal, R.; Reinhardt, B.; Renné, D.; Sengupta, M.; Wald, L.; Wilbert, S. Direct Normal Irradiance Related Definitions and Applications: The Circumsolar Issue. *Solar Energy* **2014**, *110*, 561–577. <https://doi.org/10.1016/j.solener.2014.10.001>.
193. Lindberg, O.; Lingfors, D. Oversizing Co-Located wind and Solar Parks to Increase the Capacity Factor. In *21st Wind & Solar Integration Workshop (WIW 2022)*; 2022; Vol. 2022, pp 546–552. <https://doi.org/10.1049/icp.2022.2823>.
194. Grossmann, W.; Grossmann, I.; Steininger, K. W. Solar Electricity Supply Isolines of Generation Capacity and Storage. *Proceedings of the National Academy of Sciences* **2015**, *112* (12), 3663–3668. <https://doi.org/10.1073/pnas.1316781112>.
195. Strickland, J. Space Solar vs Base Load Ground Solar and Wind Power. *Online Journal of Space Communication* **2021**, *9* (16).
196. Marzouk, O. A. Validating a Model for Bluff-Body Burners Using the HM1 Turbulent Nonpremixed Flame. *Journal of Advanced Thermal Science Research* **2016**, *3* (1), 12–23. <https://doi.org/10.15377/2409-5826.2016.03.01.2>.
197. Innovation Norway. *Innovation Norway / Conversion Guidelines - Greenhouse Gas Emissions*; Innovation Norway: Oslo, Norway, 2019; pp 1–3. <https://www.eeagrants.gov.pt/media/2776/conversion-guidelines.pdf> (accessed 2025-08-25).
198. Kvenvolden, K. A. A Review of the Geochemistry of Methane in Natural Gas Hydrate. *Organic Geochemistry* **1995**, *23* (11), 997–1008. [https://doi.org/10.1016/0146-6380\(96\)00002-2](https://doi.org/10.1016/0146-6380(96)00002-2).
199. Didmanidze, O. N.; Afanasev, A. S.; Hakimov, R. T. Natural Gas Methane Number and Its Influence on the Gas Engine Working Process Efficiency. *Записки Горного института* **2021**, *251* (eng), 730–737.
200. Marzouk, O. A.; Huckaby, E. D. A Comparative Study of Eight Finite-Rate Chemistry Kinetics for CO/H₂ Combustion. *Engineering Applications of Computational Fluid Mechanics* **2010**, *4* (3), 331–356. <https://doi.org/10.1080/19942060.2010.11015322>.
201. Maia, J. L.; da Silva Neves, M. V. Method of Equivalent CO₂ Emissions Sources Identification and Quantification of Offshore Petroleum Production Units; OnePetro, 2010. <https://doi.org/10.2118/126699-MS>.
202. Anwar, S.; Carroll, J. J. *Carbon Dioxide Thermodynamic Properties Handbook: Covering Temperatures from -20 Degrees to 250 Degrees Celcius and Pressures up to 1000 Bar*; John Wiley & Sons: Salem, Massachusetts, USA, 2011.
203. NRG Energy. *NRG Energy / Energy conversion calculator*. NRG Energy. <https://www.nrg.com/resources/energy-tools/energy-conversion-calculator.html> (accessed 2025-08-02).
204. Marzouk, O. A.; Huckaby, E. D. Modeling Confined Jets with Particles and Swirl. In *Machine Learning and Systems Engineering*; Ao, S.-I., Rieger, B., Amouzegar, M. A., Eds.; Lecture Notes in Electrical Engineering; Springer Netherlands: Dordrecht, Netherlands, 2010; Vol. 68, pp 243–256. https://doi.org/10.1007/978-90-481-9419-3_19.
205. Marzouk, O. A. InvSim Algorithm for Pre-Computing Airplane Flight Controls in Limited-Range Autonomous Missions, and Demonstration via Double-Roll Maneuver of Mirage III Fighters. *Scientific Reports* **2025**, *15*, 23382. <https://doi.org/10.1038/s41598-025-07639-6>.
206. de Obeso, J. C.; Awolayo, A. N.; Nightingale, M. J.; Tan, C.; Tutolo, B. M. Experimental Study on Plagioclase Dissolution Rates at Conditions Relevant to Mineral Carbonation of Seafloor Basalts. *Chemical Geology* **2023**, *620*, 121348. <https://doi.org/10.1016/j.chemgeo.2023.121348>.
207. GlassPoint. *Map of the Amal Oil Field in Oman*. https://images.squarespace-cdn.com/content/v1/622ba70eb380531fbf6cb5df/59876962-14d9-4f99-9a6d-b0ada0043a4b/miraah_map.jpg (accessed 2025-05-22).
208. Google. *Google Maps / Amal Oil Field*. Google Maps. <https://maps.app.goo.gl/WRdqNukjoiUs4RFt6> (accessed 2025-08-02).
209. OSMF, [OpenStreetMap Foundation]. *OpenStreetMap / Miraah Solar Farm*. OpenStreetMap. <https://www.openstreetmap.org/#map=17/18.349281/55.684590> (accessed 2025-08-02).

210. OSMF, [OpenStreetMap Foundation]. *OpenStreetMap / Copyright and License - Open Data Commons Open Database License (ODbL)*. OpenStreetMap. <https://www.openstreetmap.org/copyright> (accessed 2025-07-31).
211. GlassPoint. *Sketch of looped enclosed parabolic troughs*. <https://images.squarespace-cdn.com/content/v1/622ba70eb380531fbf6cb5df/c13e3a89-4a12-460b-bfaa-da0a71f3284a/tech1.jpg> (accessed 2025-05-24).
212. GlassPoint. *Sketch illustrating the structural advantage (wind protection) of enclosed troughs compared to open troughs*. <https://images.squarespace-cdn.com/content/v1/622ba70eb380531fbf6cb5df/e732593b-4f97-4cfd-8c3d-877227f7a193/wind.jpg> (accessed 2025-05-24).
213. Zhang, Z.; Sun, J.; Wang, L.; Wei, J. J. Multiphysics-Coupled Study of Wind Load Effects on Optical Performance of Parabolic Trough Collector. *Solar Energy* **2020**, *207*, 1078–1087. <https://doi.org/10.1016/j.solener.2020.06.107>.
214. Natraj; Rao, B. N.; Reddy, K. S. Wind Load and Structural Analysis for Standalone Solar Parabolic Trough Collector. *Renewable Energy* **2021**, *173*, 688–703. <https://doi.org/10.1016/j.renene.2021.04.007>.
215. GlassPoint. *Comparison of area needs for PV solar system solar tower system or open trough, and enclosed parabolic troughs*. <https://images.squarespace-cdn.com/content/v1/622ba70eb380531fbf6cb5df/225ab3da-e05a-488b-901f-b90f65a1a5ac/glasspoint-scale-graphic-revised.png> (accessed 2025-05-24).
216. Das, P.; V.p., C. A Review on Recent Advances in Hybrid Solar Updraft Tower Plants: Challenges and Future Aspects. *Sustainable Energy Technologies and Assessments* **2023**, *55*, 102978. <https://doi.org/10.1016/j.seta.2022.102978>.
217. Zhou, X.; Xu, Y. Solar Updraft Tower Power Generation. *Solar Energy* **2016**, *128*, 95–125. <https://doi.org/10.1016/j.solener.2014.06.029>.
218. Liang, Y.; Wang, D.; Li, Y.; Zhang, Q.; Suolang, B.; Yuan, X.; Liu, Y. Novel Approach to Remote Rural Heating: Direct Coupled Photovoltaic Electric Heater Underfloor Heating System with Phase Change Materials. *Applied Thermal Engineering* **2024**, *250*, 123525. <https://doi.org/10.1016/j.applthermaleng.2024.123525>.
219. GlassPoint. *Photo of the Amal I project in Oman*. <https://images.squarespace-cdn.com/content/v1/622ba70eb380531fbf6cb5df/1647980305001-LC69P8W8OWNV4OCSF1AD/project2.jpg> (accessed 2025-05-24).
220. GlassPoint. *Photo of the Amal I greenhouse in Oman*. <https://images.squarespace-cdn.com/content/v1/622ba70eb380531fbf6cb5df/a5903cf7-be4d-41f6-95fa-441bc534c460/GlassPoint-PDO-13.jpg> (accessed 2025-05-24).
221. PVsyst. *PVsyst / GCR - Ground coverage Ratio*. <https://www.pvsyst.com/help-pvsyst7/gcr.htm> (accessed 2025-08-02).
222. Jensen, A. R.; Sifnaios, I. Modeling, Validation, and Analysis of a Concentrating Solar Collector Field Integrated with a District Heating Network. *Solar* **2022**, *2* (2), 234–250. <https://doi.org/10.3390/solar2020013>.
223. GlassPoint. *Photo of the Amal II greenhouse in Oman*. https://images.squarespace-cdn.com/content/622ba70eb380531fbf6cb5df/1647980963994-D2FX6CA6KIDJHJ7EL260/Advance_RD.jpg (accessed 2025-05-24).
224. GlassPoint. *Photo of the night installation at the Amal II project in Oman*. https://images.squarespace-cdn.com/content/v1/622ba70eb380531fbf6cb5df/a3f25ef3-1760-47fd-b34f-6b2d63716b3b/Advance_RD2.jpg (accessed 2025-05-24).
225. *Google Maps / Miraah Project*. Google Maps. <https://maps.app.goo.gl/ZpMJJPj7A2S2ZSNZL6> (accessed 2025-08-02).
226. GlassPoint. *Aerial drone photo of the Miraah project in Oman*. https://images.squarespace-cdn.com/content/v1/622ba70eb380531fbf6cb5df/91913927-47bf-43ab-af89-ce55b5ff5bce/Miraah_drone.jpg (accessed 2025-05-24).
227. GlassPoint. *Front photo of the Miraah project in Oman*. https://images.squarespace-cdn.com/content/622ba70eb380531fbf6cb5df/1647368082815-T4QPLQM1BZGL3R2KXU2W/miraah_hero.jpg (accessed 2025-05-24).

228. Google. *Google / Brand Resource Center -Products and Services - Geo Guidelines*. Brand Resource Center. <https://about.google/brand-resource-center/products-and-services/geo-guidelines> (accessed 2025-08-02).
229. DOE, [United States Department of Energy]. *DOE / Geothermal Basics (and footprint comparison for different power technologies)*. <https://www.energy.gov/eere/geothermal/geothermal-basics> (accessed 2025-06-27).
230. Hosseini, M.; Bagheri, H. Improving the Resolution of Solar Energy Potential Maps Derived from Global DSMs for Rooftop Solar Panel Placement Using Deep Learning. *Heliyon* **2025**, *11* (1). <https://doi.org/10.1016/j.heliyon.2024.e41193>.
231. Szewczyk, R. Management of Solar Energy. *Geomatics, Landmanagement and Landscape* **2016**, no. 1. <https://doi.org/10.15576/GLL/2016.1.95>.
232. Bierman, B.; O'Donnell, J.; Burke, R.; McCormick, M.; Lindsay, W. Construction of an Enclosed Trough EOR System in South Oman. *Energy Procedia* **2014**, *49*, 1756–1765. <https://doi.org/10.1016/j.egypro.2014.03.186>.
233. Munirasu, S.; Haija, M. A.; Banat, F. Use of Membrane Technology for Oil Field and Refinery Produced Water Treatment—A Review. *Process Safety and Environmental Protection* **2016**, *100*, 183–202. <https://doi.org/10.1016/j.psep.2016.01.010>.
234. Adjovu, G. E.; Stephen, H.; James, D.; Ahmad, S. Measurement of Total Dissolved Solids and Total Suspended Solids in Water Systems: A Review of the Issues, Conventional, and Remote Sensing Techniques. *Remote Sensing* **2023**, *15* (14), 3534. <https://doi.org/10.3390/rs15143534>.
235. Heijerick, D. G.; Janssen, C. R.; Coen, W. M. D. The Combined Effects of Hardness, pH, and Dissolved Organic Carbon on the Chronic Toxicity of Zn to *D. Magna*: Development of a Surface Response Model. *Arch. Environ. Contam. Toxicol.* **2003**, *44* (2), 0210–0217. <https://doi.org/10.1007/s00244-002-2010-9>.
236. Scheuer, F.; Souza, M. P. de; Sterzelecki, F. C.; Cipriano, F. dos S.; Cerqueira, V. R.; Martins, M. L. Effect of total hardness of water on juvenile mullets (*Mugil Liza*) raised in fresh water. *Acta Veterinaria Brasilica* **2023**, *17* (1). <https://doi.org/10.21708/avb.2023.17.1.11082>.
237. Rashid, K. H.; Khadom, A. A. Sodium Sulfite as an Oxygen Scavenger for the Corrosion Control of Mild Steel in Petroleum Refinery Wastewater: Optimization, Mathematical Modeling, Surface Morphology and Reaction Kinetics Studies. *Reac Kinet Mech Cat* **2020**, *129* (2), 1027–1046. <https://doi.org/10.1007/s11144-020-01738-3>.
238. Javaherdashti, R.; Nwaoha, C.; Tan, H. *Corrosion and Materials in the Oil and Gas Industries*; CRC Press: Boca Raton, Florida, USA, 2016.
239. Marzouk, O. A. Cantera-Based Python Computer Program for Solving Steam Power Cycles with Superheating. *International Journal of Emerging Technology and Advanced Engineering* **2023**, *13* (3), 63–73.
240. Redowan, M.; Sami, T. M.; Islam, A. Design and Implementation of Solar Heater System. Thesis, Bachelor of Science in Electrical and Electronic Engineering, BRAC University, Dhaka, Bangladesh, 2016. <http://hdl.handle.net/10361/7727> (accessed 2025-08-03).
241. Biencinto, M.; González, L.; Valenzuela, L. Using Time-Windowed Solar Radiation Profiles to Assess the Daily Uncertainty of Solar Thermal Electricity Production Forecasts. *Journal of Cleaner Production* **2022**, *379*, 134821. <https://doi.org/10.1016/j.jclepro.2022.134821>.
242. Marzouk, O. A. Airfoil Design Using Genetic Algorithms. In *The 2007 International Conference on Scientific Computing (CSC'07), The 2007 World Congress in Computer Science, Computer Engineering, and Applied Computing (WORLDCOMP'07)*; CSREA Press: Las Vegas, Nevada, USA, 2007; pp 127–132.
243. Azzouzi, M. Control of Solar Water Heater Design. In *2011 10th International Conference on Environment and Electrical Engineering*; 2011; pp 1–5. <https://doi.org/10.1109/EEEIC.2011.5874684>.
244. Marzouk, O. A. Flow Control Using Bifrequency Motion. *Theoretical and Computational Fluid Dynamics* **2011**, *25* (6), 381–405. <https://doi.org/10.1007/s00162-010-0206-6>.
245. Alaskaree, E. H.; Breesam, Y. F. The Impact of Electronic Control Systems on Improving the Performance of the Solar Heater. *Engineering and Technology Journal* **2024**, *42* (7), 869–884.
246. Zou, Y.; Li, C. A Hydraulically Activated Power Launching Method for Pigs for Gas-Gathering Pipeline Networks in Gas Fields. *Journal of Pipeline Systems Engineering and Practice* **2022**, *13* (2), 04022007. [https://doi.org/10.1061/\(ASCE\)PS.1949-1204.0000639](https://doi.org/10.1061/(ASCE)PS.1949-1204.0000639).

247. Beavers, J.; Bubenik, T. A. 12 - Stress Corrosion Cracking. In *Trends in Oil and Gas Corrosion Research and Technologies*; El-Sherik, A. M., Ed.; Woodhead Publishing Series in Energy; Woodhead Publishing: Boston, 2017; pp 295–314. <https://doi.org/10.1016/B978-0-08-101105-8.00012-7>.
248. Katona, R. M.; Taylor, J. M.; McCreedy, T. A.; Bryan, C. R.; Schaller, R. F. Towards Understanding Stress Corrosion Cracking of Austenitic Stainless Steels Exposed to Realistic Sea Salt Brines. *Corrosion Science* **2024**, *232*, 111992. <https://doi.org/10.1016/j.corsci.2024.111992>.
249. SSINA, [Specialty Steel Industry of North America]. *SSINA / Chloride Stress Corrosion Cracking*. <https://www.ssina.com/education/corrosion/chloride-stress-corrosion-cracking/> (accessed 2025-08-03).
250. Venkatramani, A. V.; Okuno, R. Steam-Oil Ratio in Steam-Solvent Coinjection Simulation for Homogeneous and Heterogeneous Bitumen Reservoirs. *J. Energy Resour. Technol* **2018**, *140* (112903). <https://doi.org/10.1115/1.4040529>.
251. Ighalo, J. O.; Adeniyi, A. G. Factor Effects and Interactions in Steam Reforming of Biomass Bio-Oil. *Chem. Pap.* **2020**, *74* (5), 1459–1470. <https://doi.org/10.1007/s11696-019-00996-3>.
252. Hart, A.; Leeke, G.; Greaves, M.; Wood, J. Downhole Heavy Crude Oil Upgrading Using CAPRI: Effect of Steam upon Upgrading and Coke Formation. *Energy Fuels* **2014**, *28* (3), 1811–1819. <https://doi.org/10.1021/ef402300k>.
253. SLB, [Schlumberger Limited]. *SLB / Steam-Oil Ratio*. https://glossary.slb.com/terms/s/steam-oil_ratio (accessed 2025-10-31).
254. GER, [General Energy Recovery Inc.]. *GER / Steaming – Reducing Water Usage Through Improved Steam-to-Oil Ratio (SOR)*. https://www.geri.com/news/steam_to_oil_reduced_water_usage/ (accessed 2025-10-31).
255. Goyal, K. L.; Kumar, S. Chapter 11 Steamflooding for Enhanced Oil Recovery. In *Developments in Petroleum Science*; Donaldson, E. C., Chilingarian, G. V., Yen, T. F., Eds.; Enhanced Oil Recovery, II; Elsevier, 1989; Vol. 17, pp 317–349. [https://doi.org/10.1016/S0376-7361\(08\)70463-1](https://doi.org/10.1016/S0376-7361(08)70463-1).
256. Nie, R.-S.; Wang, Y.-M.; Kang, Y.-L.; Jia, Y.-L. A Steam Rising Model of Steam-Assisted Gravity Drainage Production for Heavy Oil Reservoirs. *Energy Exploration & Exploitation* **2020**, *38* (4), 801–818. <https://doi.org/10.1177/0144598719897178>.
257. Adibhatla, S.; Kaushik, S. C. Energy, Exergy and Economic (3E) Analysis of Integrated Solar Direct Steam Generation Combined Cycle Power Plant. *Sustainable Energy Technologies and Assessments* **2017**, *20*, 88–97. <https://doi.org/10.1016/j.seta.2017.01.002>.
258. Zhang, H.; Baeyens, J.; Cáceres, G.; Degève, J.; Lv, Y. Thermal Energy Storage: Recent Developments and Practical Aspects. *Progress in Energy and Combustion Science* **2016**, *53*, 1–40. <https://doi.org/10.1016/j.pecs.2015.10.003>.
259. Cabeza, L. F. 2 - Advances in Thermal Energy Storage Systems: Methods and Applications. In *Advances in Thermal Energy Storage Systems (Second Edition)*; Cabeza, L. F., Ed.; Woodhead Publishing Series in Energy; Woodhead Publishing, 2021; pp 37–54. <https://doi.org/10.1016/B978-0-12-819885-8.00002-4>.
260. Werner, S. International Review of District Heating and Cooling. *Energy* **2017**, *137*, 617–631. <https://doi.org/10.1016/j.energy.2017.04.045>.
261. Lund, H.; Østergaard, P. A.; Chang, M.; Werner, S.; Svendsen, S.; Sorknæs, P.; Thorsen, J. E.; Hvelplund, F.; Mortensen, B. O. G.; Mathiesen, B. V.; Bojesen, C.; Duic, N.; Zhang, X.; Möller, B. The Status of 4th Generation District Heating: Research and Results. *Energy* **2018**, *164*, 147–159. <https://doi.org/10.1016/j.energy.2018.08.206>.
262. Karni, J. SOLAR-THERMAL POWER GENERATION. *Annual Review of Heat Transfer* **2012**, *15*. <https://doi.org/10.1615/AnnualRevHeatTransfer.2012004925>.
263. Tsoutsos, T.; Gekas, V.; Marketaki, K. Technical and Economical Evaluation of Solar Thermal Power Generation. *Renewable Energy* **2003**, *28* (6), 873–886. [https://doi.org/10.1016/S0960-1481\(02\)00152-0](https://doi.org/10.1016/S0960-1481(02)00152-0).
264. Sharma, C.; Sharma, A. K.; Mullick, S. C.; Kandpal, T. C. Assessment of Solar Thermal Power Generation Potential in India. *Renewable and Sustainable Energy Reviews* **2015**, *42*, 902–912. <https://doi.org/10.1016/j.rser.2014.10.059>.
265. Kamfa, I.; Fluch, J.; Bartali, R.; Baker, D. Solar-Thermal Driven Drying Technologies for Large-Scale Industrial Applications: State of the Art, Gaps, and Opportunities. *International Journal of Energy Research* **2020**, *44* (13), 9864–9888. <https://doi.org/10.1002/er.5622>.

266. Eswara, A. R.; Ramakrishnarao, M. Solar Energy in Food Processing—a Critical Appraisal. *J Food Sci Technol* **2013**, *50* (2), 209–227. <https://doi.org/10.1007/s13197-012-0739-3>.
267. Saxena, A.; Goel, V.; Karakilcik, M. Solar Food Processing and Cooking Methodologies. In *Applications of Solar Energy*; Tyagi, H., Agarwal, A. K., Chakraborty, P. R., Powar, S., Eds.; Springer: Singapore, 2018; pp 251–294. https://doi.org/10.1007/978-981-10-7206-2_13.
268. Lee, M.; Hong, T.; Koo, C. An Economic Impact Analysis of State Solar Incentives for Improving Financial Performance of Residential Solar Photovoltaic Systems in the United States. *Renewable and Sustainable Energy Reviews* **2016**, *58*, 590–607. <https://doi.org/10.1016/j.rser.2015.12.297>.
269. Sarzynski, A.; Larrieu, J.; Shrimali, G. The Impact of State Financial Incentives on Market Deployment of Solar Technology. *Energy Policy* **2012**, *46*, 550–557. <https://doi.org/10.1016/j.enpol.2012.04.032>.
270. Matisoff, D. C.; Johnson, E. P. The Comparative Effectiveness of Residential Solar Incentives. *Energy Policy* **2017**, *108*, 44–54. <https://doi.org/10.1016/j.enpol.2017.05.032>.

Disclaimer/Publisher’s Note: The statements, opinions and data contained in all publications are solely those of the individual author(s) and contributor(s) and not of MDPI and/or the editor(s). MDPI and/or the editor(s) disclaim responsibility for any injury to people or property resulting from any ideas, methods, instructions or products referred to in the content.